APPROACH TO CRITICAL IN CROCUS

1. INTRODUCTION

In order to understand the process of achieving a critical configuration with a reactor, it is important to define basic terms such as the start-up neutron source, the subcritical multiplication, the effective multiplication factor and the reactivity.

In a nuclear reactor, apart from the neutron production via fission reactions, neutrons are also produced as a result of certain other nuclear reactions and these are usually referred to as source neutrons. These neutrons provide useful information during shutdown and start-up sequences, using neutron-sensitive monitors placed in and around the reactor. Since changes in the neutron population reflect on the state of the reactor, it is important to verify that there is sufficient neutron flux (also when the reactor is shutdown), which can be detected by an appropriate choice of neutron detectors. The source neutrons needed for the purpose can be "intrinsic" and/or "external". A brief introduction is given below about the nature of such sources.

1.1 Intrinsic neutron source

Several heavy nuclides present in the reactor undergo spontaneous fission leading to the release of neutrons. A list of isotopes along with their specific neutron yields is given in Table 1.

Table 1 Spontaneous fission neutron sources.

Nuclide	Half-life of spontaneous fission source [years]	Decay constant [s^{-1}]	Neutron production [$n.s^{-1}.g^{-1}$]
^{232}Th	1.0E+18	2.196E-26	1.20E-4
^{233}U	1.0E+15	2.196E-23	1.25E-1
^{235}U	1.8E+17	1.220E-25	7.57E-4
^{238}U	8.0E+15	2.745E-24	1.86E-2
^{239}Pu	5.5E+15	3.994E-24	3.21E-2
^{240}Pu	1.2E+11	1.830E-19	1.47E+3
^{252}Cf	66.0	3.328E-10	3.02E+12

Also, some of the heavier isotopes of uranium and plutonium emit alpha particles and, when boron is present in the fuel, these can interact with ^{11}B (80.1% of natural boron) to produce neutrons from the following reaction:

$$ {}^{11}_{5}B + {}^{4}_{2}He \Rightarrow {}^{14}_{7}N + {}^{1}_{0}n \qquad (1) $$

Neutrons may also be produced by the following gamma interaction with deuterium.

$$ {}^{2}_{1}H + \gamma \Rightarrow {}^{1}_{1}H + {}^{1}_{0}n \qquad (2) $$

There are abundant high energy photons that are produced from the fission products, and their intensity is governed by the operating power level and the duration of the reactor operation. The atom % of deuterium in the water ranges from 0.015% for a light water reactor to 99.8% for a heavy water reactor. Since the neutron emission is essentially due to the production of gamma rays, the source strength for such a source depends on the operational and shutdown history of the reactor.

1.2 External neutron source

Since the neutron source strength due to intrinsic sources is quite small in low-power reactors, it becomes essential to use an external neutron source to bring the reactor to critical in a reasonable period of time. All experimental reactors have provision for introduction of an external neutron source into the reactor, with the sole objective of being able to quantify the shutdown levels properly with the help of neutron-sensitive monitors. The external neutron source is usually withdrawn back into its containment outside the reactor, once criticality has been achieved.

Among the standard external sources, ^{252}Cf (spontaneous-fission source) is an important one. It emits about 3.0E+12 n/s per gram of the nuclide. However, it is quite expensive and also has certain other drawbacks, viz. a relatively short half-life and the emission of high energy gamma radiation.

Several commercial neutron sources are based on the (α,n) reaction with beryllium as given below:

$$^{9}_{4}Be + {}^{4}_{2}He \rightarrow {}^{12}_{6}C + {}^{1}_{0}n \qquad (3)$$

These sources consist of metallic beryllium uniformly mixed with alpha emitter such as ^{210}Po, ^{226}Ra, ^{238}Pu and ^{241}Am. Another commonly available neutron source is based on the (γ, n) reaction given below:

$$^{2}_{1}H + \gamma \Rightarrow {}^{1}_{1}H + {}^{1}_{0}n \qquad (4)$$

The gamma radiation is usually obtained from a radioisotope such as ^{124}Sb (which can be produced in a reactor from neutron capture in ^{123}Sb). Unlike sources based on (α,n) reaction, photon-based sources do not need to be uniformly mixed. In fact, some designs employ a gamma source contained in a capsule, which is surrounded by a sleeve of beryllium.

1.3 Subcritical multiplication

When a neutron source is placed in a block of moderating material such as graphite, there will be a steady-state neutron flux (or density) distribution, which will depend upon the strength of the neutron source, the absorption of neutrons in the graphite and the neutron leakage. When a fissile material is added to the moderator, there will be an increase in the neutron flux at any given point in the assembly. This will depend upon the kind and amount of fissile material added, as also the geometrical arrangement used for the materials.

The multiplication *M*, of a subcritical fissile assembly of the above type, is defined as the ratio between the thermal neutron flux due to both the primary source and fission, and that due to the primary source alone. If a neutron detector placed in the assembly is assumed to measure, in the presence of a neutron source, a count rate (cps) proportional to the neutron flux, then the neutron multiplication *M* of the system is given by:

$$M = \text{cps with fuel / cps without fuel} = I_{wf}/I_{nf} \qquad (5)$$

where I_{wf} and I_{nf} denote neutron flux (or detector response) with and without the fissile material, respectively.

1.4 Effective multiplication factor

In reactor experiments, the spatial and energy distributions of greatest significance are those characteristics of the critical reactor, in which the effective multiplication factor, k or k_{eff} (defined as the ratio of the number of neutrons in one generation to that in the preceding generation), is unity.

In the case of a subcritical assembly with a neutron source, the distributions are more complex. However, in any case, the subcritical multiplication M can be related to the assembly's k value, which is less than 1. Thus, S source neutrons result in kS, k^2S, k^3S... neutrons in the 1st, 2nd, 3rd… generations, respectively. Hence, the M value for the assembly is given by:

$$M = \frac{S(1 + k + k^2 + k^3 + k^4 .....)}{S} = \frac{1}{1-k} \tag{6}$$

There are certain practical difficulties to obtain an accurate value of k from a multiplication experiment, e.g. difficulties in distributing the source in the "normal mode" and in measuring the neutron count rates throughout the assembly, particularly when the measurements are required for a series of subcritical states.

Instead, one adopts an empirical approach, the count rate, $C_{wf}(k)$ of a neutron detector placed in or near the assembly being taken as a relative measure of the neutron population and being determined as a function of the corresponding k value. The multiplication M, as observed by such a detector, is then given by:

$$M_{obs} = C_{wf}(k)/C_{nf} \tag{7}$$

where C_{wf} and C_{nf} correspond to the count rates with and without the fissile material, respectively.

1.5 Reactivity

For completeness, one needs to recall that the concept of a critical configuration can also be defined in terms of reactivity (ρ), defined by:

$$\rho = \frac{\delta k}{k_{eff}} = \frac{k_{eff} - 1}{k_{eff}} \tag{8}$$

Clearly, the reactivity is zero for a critical reactor, negative for a subcritical assembly and positive for a supercritical reactor. It is common to express reactivity in pcm units (1 pcm = 10-5). For example, the maximum possible positive reactivity in CROCUS is +200 pcm, i.e. $\rho = 0.002$.

1.6 Approach-to-critical experiment

As indicated earlier, there are certain difficulties in relating M_{obs} to the true subcritical multiplication M. These arise from the sensitivity of the spatial and energy distributions of the neutron flux to k_{eff}, source location and assembly geometry. This means that the observed multiplication will depend on the position of the detector, its energy response and details of the experimental conditions. It is known, however, that for approximately $k > 0.95$ and depending on the system, the neutron spectrum remains nearly constant and the flux increases almost proportionately throughout the reactor as k is increased.

Despite its drawbacks as a method to measure k, the multiplication experiment is performed routinely in the context of the safe loading, or "approach to critical", of any given multiplying assembly being

brought to critical for the first time. Usually, an approach to critical is achieved by loading fuel material in small steps. It is, however, possible to demonstrate the basic principles by increasing the k-value of a subcritical reactor in relation to a change in the moderator level or the withdrawal of a control rod. In an approach-to-critical experiment, the basic relations employed are those of Equations (6 & 7):

$$M_{obs} = \frac{C_{wf}(k)}{C_{nf}} = \frac{1}{1-k} \qquad (9)$$

From the definition of k, it is evident that, for $k < 1$, the number of fissions, and hence neutron flux decreases from one generation to the next, the chain reaction being subcritical. In an approach-to-critical experiment, i.e. for achieving $k = 1$, the value of k needs to be changed slowly from a low value, while tracking the response of the detector which is proportional to the factor M_{obs} of Equation (9). By plotting $1/M_{obs}$, or $1/C_{wf}(k)$ (C_{nf} being constant), against the amount of fuel loaded and extrapolating the value to achieve the loading corresponding to $1/M_{obs} = 1/C_{wf}(k) = 0$, one gets the critical configuration. Clearly, as mentioned, one may be employing a different means of varying k, such as change in moderator level or control rod position. The basic procedural steps, however, are similar

An approach-to-critical experiment needs to be done extremely carefully, ensuring that, under any circumstances, criticality is not reached inadvertently. Such a situation could possibly arise because the slope of the plots obtained during an approach-to-critical experiment can have different shapes depending upon the choice of the location of the detector. As illustration, representative results are discussed for an Argonaut multiplication assembly, a cut-away view of which is shown in Fig. 1.

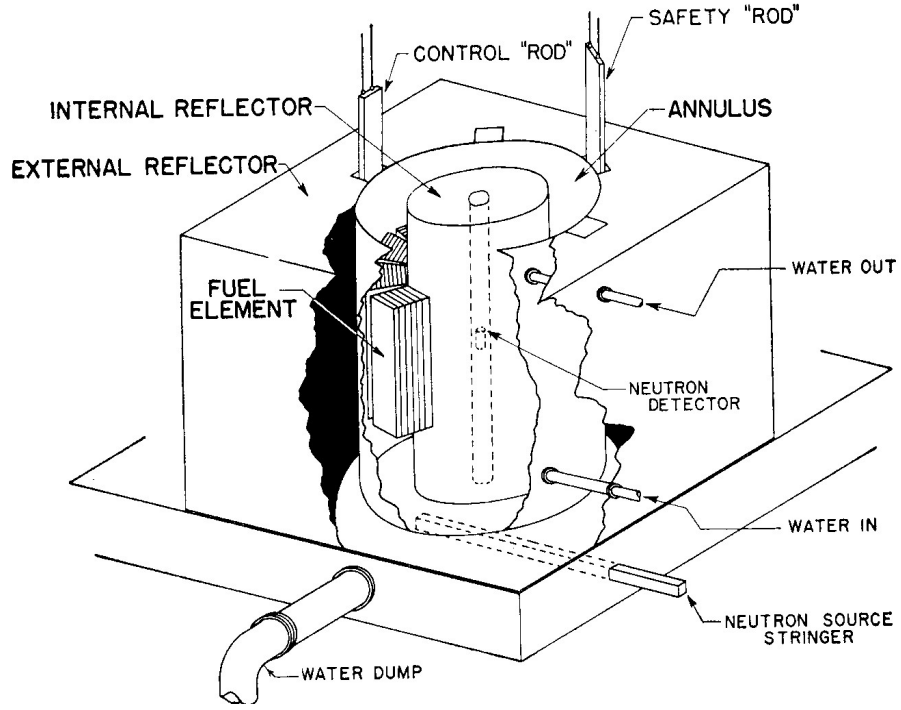

Fig. 1: Schematic view of the Argonaut multiplication assembly.

Fig. 2 illustrates the results of a representative approach-to-critical experiment, carried out using BF_3 detectors, the inverse count rates having being plotted for three different BF_3 detector positions. While an ideal curve would be a linear one, it can be seen that plot No. 1 & 3 are particularly "dangerous" for extrapolating to the critical mass unless one has carried out measurements with small loading steps till at least about 1.5 kg of ^{235}U (in this particular example). Plot No. 2, which reflects the neutron flux at a location closer to the fissile material, in comparison to the other locations, gives a significantly better description for extrapolation from a loading onwards of about 1.0 kg ^{235}U.

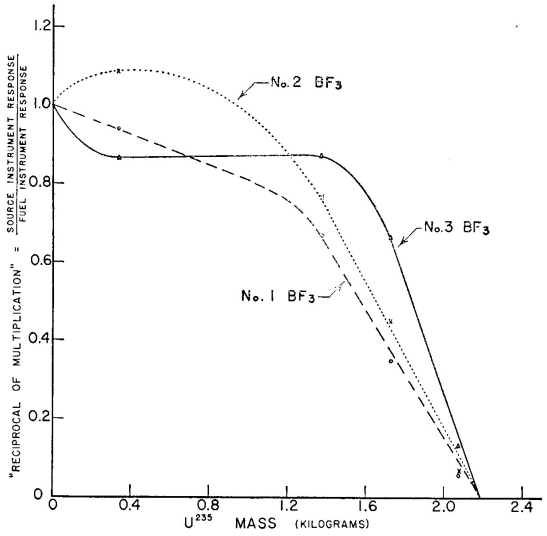

Fig. 2: An approach-to-critical experiment with the Argonaut multiplication assembly using BF3 detectors; 1) detector located at top of the central hole; 2) detector outside the reflector on the fuel side; 3) detector about 120 cm above the central hole.

A typical, "well-behaved" inverse-counts plot is shown in Fig. 3, the prediction of the critical loading here being seen to be relatively reliable, although small-step measurements, even in this case, remain essential till quite near to the end. An often used prescription for calculating the next "loading step" during an approach to critical is to implement no more than about one-third of the increment predicted (to zero inverse counts) at any given stage [1].

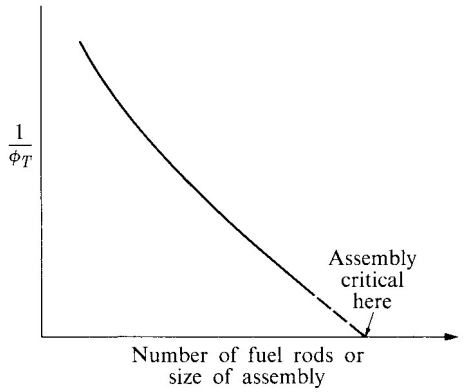

Fig. 3: A "well-behaved" inverse counts plot during an approach-to-critical experiment.

When a nuclear reactor is built, one needs more than just the critical mass of fissile material. For a power reactor, the excess reactivity is required to compensate for burnup effects and ensure a certain cycle length of steady-state operation for the loaded fuel. Even in the case of a zero-power reactor such as CROCUS, some slight excess reactivity is needed in order to be able to increase the neutron flux, i.e. establish different low-power values. In all case, the excess reactivity has to be compensated, and this is usually done by introducing absorbing material in the form of control or regulating rods.

In the CROCUS facility, there are two types of approach-to-critical experiments which are possible. The increase of the moderator (water) level, without any use of the control rods, is clearly one possible means of varying the k_{eff} value. The other possibility is to have, at the start of the experiment, at least one of the control rods fully inserted and the moderator level at a specific height. The k_{eff} variation of the reactor can then be carried out in terms of small-step withdrawals of the inserted control rod, in order to extrapolate to zero inverse-counts for the critical control-rod position.

In the present context, the approach to critical for CROCUS reactor will be carried out by varying the water level.

2. PURPOSE

The purposes of this experiment are:

- Assessment of the suitability of each detector and its location for realistic prediction of the critical height.
- Prediction of the steps of the approach to critical using the inverse counts plot
- Determination of the critical water level with uncertainties.

3. SAFETY MEASURES

In order to work under the standard regulations for control of radiation exposure the safety measures during the experiment are:

- Personal dosimeter for each participant of the experiment (teachers, students and reactor operators) provided by the radiation safety group.
- Drinking and eating is not allowed in the control area.
- Each intended change in reactivity should be carefully evaluated and communicated to the reactor operator.
- The change in water level is to be carried out only by the reactor operator.
- Following a water level change, sufficient time (about 10 minutes) should be allowed for the flux to stabilise, before carrying out the data acquisition.
- The inverse-counts-vs.-water-level plot should be acquired “on-line”, in order to properly assess the next increment in water level.

4. INSTRUMENTS AND MATERIALS

This experiment measures the axial distribution of thermal neutron flux and the Cd-ratio, therefore is done in the core of a nuclear reactor. It needs the following:

- The CROCUS reactor in subcritical state (operator).
- Spillway system for a precise setting and knowledge of the water level.
- Fission (2) and ionisation (2) chambers in the periphery of the CROCUS reactor core, with associated electronics.

5. EXPERIMENTAL PROCEDURES

- Switch on the power supplies of all the associated electronic units and verify the specified settings. Switch on the PC, if needed, for data processing or for using the MCS acquisition system connected to the fission chamber.
- Make sure that the CROCUS reactor has an initial water level such that the configuration is subcritical (k_{eff} ~0.96); this is done by the reactor operator.
- Make sure the start-up Pu(α,n)Be neutron source is under the core before starting the measurements.
- Switch on the data acquisition for the fission chambers for a definite period of time. For a given measurement point, the data acquisition is initiated after a waiting time of ~10 min following the change in water level (to ensure stabilisation of the delayed neutron precursors). It is necessary to have sufficient counting statistics for each measurement point (assuming a Poisson distribution). A compromise between accuracy and measurement duration has to be found. Several series of measurements can also be used. Read the ionization current directly on the instrument.
- The water level increment in height is 10 mm in the first step. Increase the water level in steps of suitable height increase and repeat the above measurements.
- Finally, verify that the reactor is critical assuming the predicted water level. Consider the need of the source at that instant.

6. MAIN PARAMETERS MEASURED

In order to obtain the inverse-counts plot for each detector, it is necessary to collect the following data:

- Mark the water level position indicated by the spillway system.
- Collect the fission and ionisation chambers responses at each water level increase step.

7. TYPICAL REAL DATA COLLECTED

Examples of the typical real data collected:

Table 2: Experimental results for fission chambers for approach to critical with water level.

	Average count rate (counts/s)		
Water level	**Fission chamber 1**	**Fission chamber 2**	**Fission chambers combined**
910 mm	20.97 ± 0.70	20.72 ± 0.69	20.84 ± 0.59
918 mm	25.21 ± 0.22	24.29 ± 0.22	24.75 ± 0.15
926 mm	31.07 ± 0.39	30.92 ± 0.39	30.99 ± 0.23
934 mm	42.36 ± 0.46	41.32 ± 0.45	41.84 ± 0.26
942 mm	66.74 ± 0.58	65.05 ± 0.57	65.90 ± 0.33

Table 3: Experimental results for ionisation chambers for approach to critical with water level.

	Measured current (nA)	
Water Level	**Ionisation chamber 1**	**Ionisation chamber 2**
900 mm	0.18 ± 0.01	0.18 ± 0.01
910 mm	0.22 ± 0.01	0.22 ± 0.01
930 mm	0.38 ± 0.02	0.40 ± 0.02
940 mm	0.62 ± 0.02	0.64 ± 0.02

8. DATA ANALYSIS, ASSUMPTIONS AND EQUATIONS

- The subcritical multiplication M can be related to the assembly's k value, which is less than 1. Thus, S source neutrons result in kS, k^2S, k^3S... neutrons in the 1st, 2nd, 3rd… generations, respectively. Hence, the M value for the assembly is given by:

$$M = \frac{S(1 + k + k^2 + k^3 + k^4 .....)}{S} = \frac{1}{1-k}$$

- One adopts an empirical approach, the count rate, $C_{wf(k)}$ of a neutron detector placed in or near the assembly being taken as a relative measure of the neutron population and being determined as a function of the corresponding k value. The multiplication M, as observed by such a detector, is then given by:

$$M_{obs} = \frac{C_{wf}(k)}{C_{nf}} = \frac{1}{1-k}$$

where C_{wf} and C_{nf} correspond to the count rates with and without the fissile material, respectively.

- It is also important to consider other parameters contributing to error apart from the counting statistics. More often, the data obtained need to be processed by additional steps such as addition, subtraction, multiplication and other functional manipulations, in order to arrive at the specific parameter of interest. The numerical values arising from these steps will be distributed in a way that is dependent on both the original distribution and the types of operations carried out.

- The standard deviation on a quantity u(x, y, z, …) can be derived from the standard deviation of each independent variable denoted by $\sigma_x, \sigma_y, \sigma_z ....$, using the standard error propagation formula given by:

$$\sigma_u^2 = \left(\frac{\partial u}{\partial x}\right)^2 \sigma_x^2 + \left(\frac{\partial u}{\partial y}\right)^2 \sigma_y^2 + \left(\frac{\partial u}{\partial z}\right)^2 \sigma_z^2 + ...$$

9. PRE-KNOWLEDGE REQUIRED FROM STUDENTS

The students should be familiar with following contents:

- nuclear measurements: different types of neutron detectors, basic experimental set up.
- reactor physics: neutron flux in a reactor, spatial and energetic distribution, control rod perturbations, reactivity, critical state.
- radiation protection: dose rates, limits and all aspects regarding radiological protection, necessary to perform the experience under high security standards.

10.RESULTS

The number of counts during each acquisition interval at each water level height is shown in Table 2. In reality these values do not represent the true flux in these volumes because the detectors are not 100-percent efficient. This is not too much of a concern because the count rates will later be normalized. The factors used to alter the count rates will cancel out in the normalization process and therefore the calculation is unnecessary to perform.

Reported with the counts is the standard deviation involved in their measurement, calculated by Equation (5) where $\sigma_{\bar{x}}$, is the standard deviation in the average count rate, $\bar{x}$ is the average number of counts per acquisition time, N is the number of measurement intervals, and A is the acquisition time for each measurement. Each measurement interval was converted into a rate by dividing by the acquisition time. This equation only works for averages of measurements with identical acquisition times, as was the case in this experiment.

The *1/M* curve was created by normalizing the count rates at each augmented water level to base count rate measured when the water level was at 910 mm, creating a data plot with fitted linear curves that start at y = 1 and are extrapolated to y = 0. Equation (7) shows the normalization formula for calculating *M* and Table 4 shows the values obtained for *M* for each detector, and the average of all of the detectors combined.

Table 4 *M*, multiplication factors for each water level.

Water Level	Fission Chamber 1	Fission Chamber 2	Fission Chambers Combined
910 mm	1.00	1.00	1.00
918 mm	1.20	1.16	1.19
926 mm	1.48	1.47	1.49
934 mm	2.02	1.97	2.00
942 mm	3.18	3.10	3.16

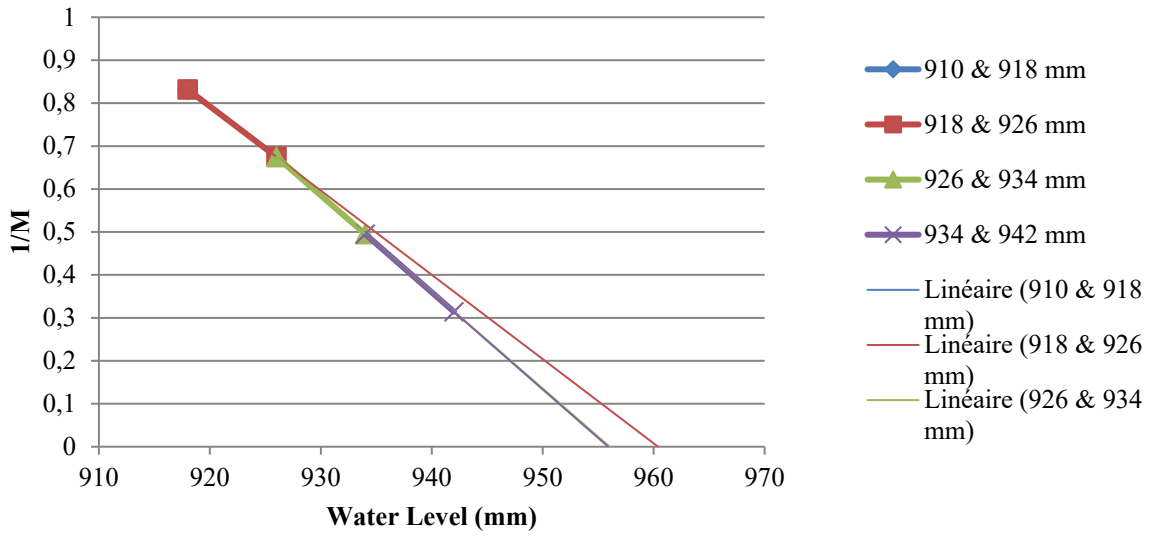

Fig. 4:Averaged and normalized *1/M* curve with extrapolated lines using averaged fission chambers measurements.

The extrapolated lines in Fig. 4 predict where the critical water level is from the values of the current and previous water levels. Only two values, the current and previous, were used for a number of reasons when creating the extrapolated *1/M* curve. The first and most important reason is that this resembles the practice performed in reactor operations. In a fuel loading procedure or reactor startup from hot, clean shutdown, it is essential that a super-critical condition is not reached. Accidental super-criticality would be a safety and regulatory disaster. Therefore the criticality of the reactor is increased by small increments, after which the new ultimate critical condition is predicted. If the increment is kept sufficiently small, the operators can be assured that the reactor will always be within their control and subcritical.

Table 5 contains the predicted critical positions of each line, calculated by solving for x in each linear equation when y is set equal to zero.

Table 5 Linear equations and predicted critical positions for the average and normalized 1/C curve.

Water Levels Used in Extrapolation (mm)	Linear Equation	Predicted Water Level at Critical (mm)
910 & 918	y = -0.021x + 20.123	958.4
918 & 926	y = -0.0196x + 18.844	961.0
926 & 934	y = -0.0225x + 21.486	955.4
934 & 942	y = -0.0226x + 21.614	956.2

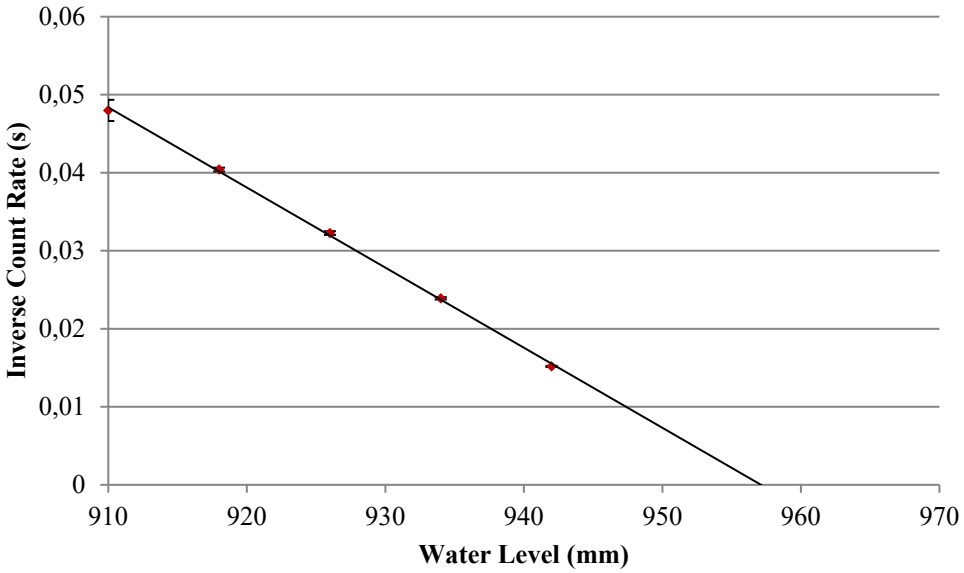

Fig. 5: 1/C curve using all measurements in extrapolation.

11.CONCLUSIONS

Multiple methods were investigated in an attempt to plot the most reliable *1/M* curve possible. Normalizing the count rates and plotting either all data points or the two most recent data points only gave comparably equivalent results to the inverse count rate plot. Considering this, in the case of CROCUS, each of these methods can be used as a valid approach.

The first few extrapolations deviated from the reference critical water level of (955.3±0.1) mm, confirmed by operator, by less than 24 pcm (~6.0 mm of water level). While approaching to criticality, the extrapolated critical position prediction began to fluctuate around (955.8±0.4) mm, within the statistical error of the experimental method. The obtained *1/M* curve confirmed the importance of taking multiple measurements, evaluating statistical errors and doing multiple predictions. The second extrapolation over-predicted the critical position of the water level to a value of 961.0 mm. If only this prediction was used and water was increased to this level without any further consideration, the reactor would have been in a supercritical state, therefore in an unstable regime.

12.REFERENCES

[1] A. E. Profio, Experimental Reactor Physics, John Wiley & sons Inc., 1976.

STABLE PERIOD MEASUREMENTS

1. INTRODUCTION

For a reactor, with an effective multiplication factor k_{eff}, or simply k, the reactivity ρ is defined by:

$$\rho = \frac{k-1}{k} \tag{1}$$

Clearly, for a critical system ($k_{eff}=1$), the reactivity is zero. If the reactor is subcritical ($k < 1$), its reactivity is negative. If it is supercritical ($k > 1$), the reactivity is positive and the neutron flux will increase exponentially, i.e. the reactor will have a positive stable period.

For the long-term operation of a power reactor, the initial built-in reactivity needs to be positive in order to be able to compensate for the k_{eff} decrease with fuel burnup. Reactor control is achieved via the insertion of neutron absorbers in the core, usually in the form of control rods, these rods being withdrawn during the course of the reactor's operation such that it can be maintained in its critical state throughout. The neutronics modelling of control rods in thermal reactors is discussed in all standard reactor physics books [1-2], considering one- or two-group diffusion theory.

Fig. 1 illustrates the influence on the neutron flux distribution of a central control rod inserted into a reactor core. The principal effect, which causes the reduction of k_{eff}, is the increase in parasitic absorptions due to the control rod insertion. However, the flux depression due to the absorption of thermal neutrons results in a certain hardening of the neutron spectrum and also in an increase in the flux gradient at the reactor core edges. Both of these changes result in a higher neutron leakage, which augments the negative reactivity effect of the control rod insertion.

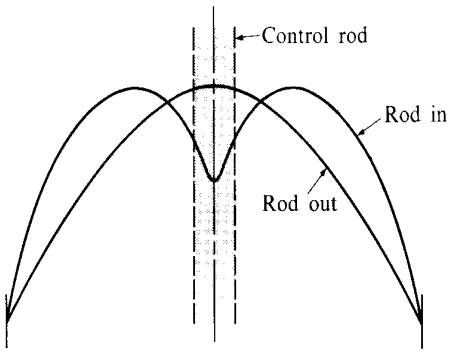

Fig. 1: A schematic of the flux in a bare reactor with ("Rod in") and without ("Rod out") a central control rod.

Thus, $d\rho/dz$ can be defined as the differential reactivity added to the system when a control rod is withdrawn by the distance dz. Then the reactivity effect corresponding to the withdrawal of the rod to a distance z_1 is given by:

$$\rho(z_1) = \int_0^{z_1} \frac{d\rho}{dz} dz \tag{2}$$

The total or integral "reactivity worth" of the control rod is the effect of its full withdrawal.

A reactor will normally have several control rods, which are classified as per their primary role. The regulating rod has a small worth, and is used for making fine adjustments in reactivity. It may be operated manually or by an automatic servomechanism. A shim rod has greater worth and is used for coarse adjustments in reactivity, e.g. to compensate for reactivity changes due to temperature, xenon poisoning or fuel burnup. Safety or shutdown rods, which are kept in fully withdrawn positions during normal operation, have significant worths, and therefore, their design allows an insertion into the core in a fraction of a second to achieve a rapid shutdown of the reactor (scram).

The worth of a given control rod depends upon its position in the reactor core, the maximum value being generally found at the centre. However, it is important to realise that "shadowing" or "anti-shadowing" effects between individual control rods might be present, depending upon their relative positions. For safety reasons, control rods are located at different positions such that their interactions are of low importance.

Methods for measuring control rod worth

There are several methods to measure the worth of a given control rod, e.g. stable (or asymptotic) period ("inverse kinetics"), rod drop, rod oscillator, sub-critical multiplication and pulsed-neutron-source techniques.

The shape of the $d\rho/dz$ curves can be estimated from perturbation theory. In the case of a weakly absorbing control rod, first-order perturbation theory may be applied. Considering the one-group, bare reactor model for a cylindrical reactor of extrapolated height *H*, the rate of change of reactivity per unit length can be written as:

$$\frac{d\rho}{dz} \approx sin^2 \frac{\pi z}{H} \tag{3}$$

where *z* is measured from the bottom of the reactor. The solution of Equation (3) follows as:

$$\rho(z) \cong \frac{\rho(H)}{2\pi}\left[\frac{2\pi z}{H} - sin\frac{2\pi z}{H}\right] \tag{4}$$

The above shape has been found to fit with a good precision, even when the perturbation is fairly large and when bare, one-group reactor theory is not strictly applicable.

It should be mentioned that it is possible to evaluate the reactivity change due to a given control rod movement, i.e. to determine the corresponding worth, by compensating the effect via the movement of another rod of known worth. This is the so-called null reactivity method and it is effective if the two rods – one being calibrated and the other serving as a reference – do not influence each other significantly.

In the current experiment, one of the two control rods of the CROCUS reactor will be calibrated via application of the 'Reactivity Equation', which relates the step change in reactivity in a given reactor to the corresponding stable period (see next section). The reactivity worth values obtained for different withdrawal steps of the control rod being calibrated will then be compared with the corresponding values provided for the second CROCUS control rod.

Stable reactor period

Hypothetical case of a system without delayed neutrons

Applying the so-called point reactor model to the hypothetical case of a reactor in which all the neutrons are considered born as prompt neutrons, the rate of increase of the neutron population is given by:

$$p(t) = p(0).\exp\left[\frac{(k_{eff} - 1)}{l} \cdot t\right] \tag{5}$$

where $P(0)$, k_{eff} and l represent the neutron population at $t=0$, the effective infinite multiplication factor and the prompt neutron lifetime, respectively. The latter is effectively a measure of the time between the birth of a neutron and its disappearance in face of absorption and leakage.

Equation (5) may be written as:

$$N_F(t) = N_F(0).e^{t/T}.p(t) = p(0).e^{t/T} \tag{6}$$

where $\tau = l/(k_{eff} - 1)$, stands for the reactor period and can be interpreted as the time resulting in the e-fold increase in reactor power or flux. A typical value for the prompt neutron lifetime in a thermal reactor is 10^{-3} s. Thus, in the hypothetical case with all neutrons assumed to be prompt, an increase of k_{eff} from 1.000 to say 1.005 would result in a reactor period of just $\tau = 0.001/0.005 = 0.2$ s, i.e. the reactor power would increase by $e^{1/0.2}=e^5=148$ every second, a clearly uncontrollable scenario. In reality, due to the presence of delayed neutrons, the rate of power increase is much slower.

Reactor with delayed neutrons

For the real case of a reactor with delayed neutrons – usually considered in 6 groups with group-specific values for the decay constant (λ_i) and the delayed-neutron fraction (β_i) – the point-kinetics equations are:

$$\frac{dP}{dt} = \frac{\rho(t)-\beta}{\Lambda}.P(t) + \sum_{i=1}^{6}[\lambda_i C_i(t)] \tag{7}$$

and

$$\frac{dC_i}{dt} + \lambda_i \cdot C_i(t) = \frac{\beta_i}{\Lambda} \cdot P(t) \tag{8}$$

where P is the neutron population, C_i is the precursor concentration for group i, and one has used the definition of reactivity, $\rho = (k_{eff} - 1)/k_{eff}$, and the prompt neutron generation time, $\Lambda = l/k_{eff}$.

The solution of the above system of coupled, linear differential equations for the case of a step change in reactivity ρ leads to an evolution of the neutron population of the type:

$$\frac{P(t)}{P(0)} = \sum_{j=1}^{j=7} B_j \cdot e^{w_j t} \tag{9}$$

where the B_j are constants and the ω_j are given by the roots of the so-called 'Reactivity Equation' or 'Inhour Equation':

$$\rho = \Lambda\varpi + \sum_{i=1}^{6} \frac{\beta_i \varpi}{\varpi + \lambda_i} \tag{10}$$

Fig. 2 is a schematic depicting the graphical solution of Equation (10) for both positive and negative ρ values. It is seen that, for the case of a positive step change in reactivity, there is just a single ω value which is positive (ω_1), all other roots being negative and thus corresponding to terms in Equation (9) which die away. The stable (positive) period for the neutron population, or flux, is $T = 1/\omega_1$. For the case of a negative step change in reactivity, all the seven roots of Equation (10) are seen to be negative. Here, since the terms in Equation (9) associated with the larger ω values die away quicker, the stable (negative) period is also simply $T = 1/\omega_1$.

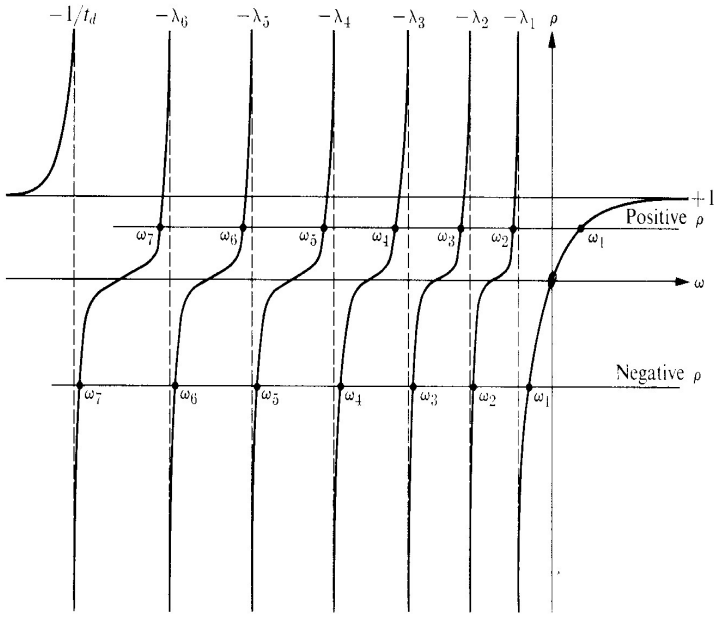

Fig. 2: A schematic of the graphical solution of the Reactivity Equation showing the seven roots for positive and negative reactivity.

Fig. 3 illustrates the evolution of the neutron flux, following a 0.001 step increase of reactivity in a ^{235}U fuelled thermal reactor [1]. The "transient region" at the beginning corresponds to the die-away of the six terms of Equation (9) which have negative ω values. It can be shown that the coefficients B_j associated with these terms are also negative, the vanishing of negative terms being the explanation why the transient region corresponds to an initial rapid increase of the flux. The slower stable rate of flux increase thereafter corresponds to the stable reactor period, $T = 1/\omega_1$.

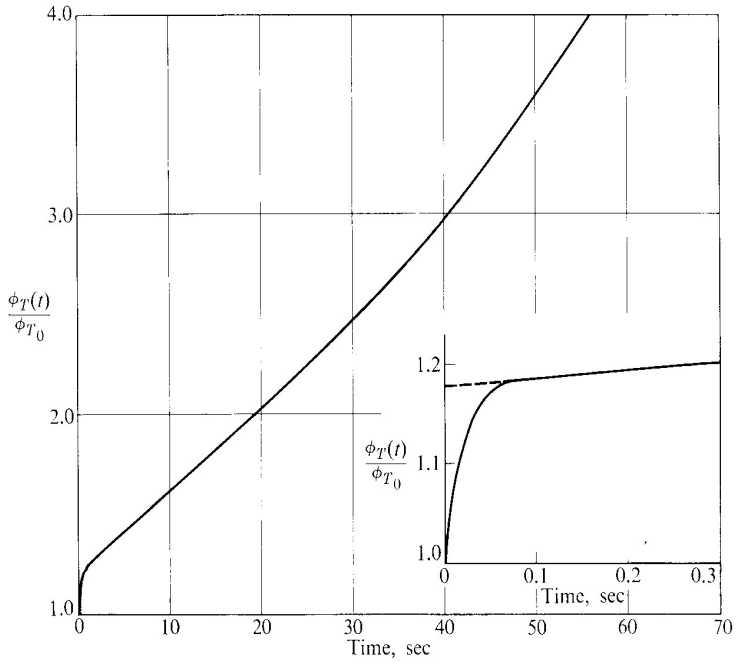

Fig. 3: Time behaviour of thermal neutron flux in infinite ^{235}U fuelled, H_2O moderated thermal reactor following step reactivity insertion of 0.001, [1].

Clearly, in the present measurements of the stable period corresponding to a given withdrawal step of one of the CROCUS control rods, it will be necessary to use an appropriate range of the time-dependent data for deducing ω_1, i.e. to ensure that the initial data points corresponding to the transient region have been exempted from the exponential fitting. The ρ value (or worth) can then be obtained by substituting the deduced ω_1 value into the Reactivity Equation, Equation (10), along with the provided kinetics parameters (Λ, λ_I, β_i) for the CROCUS reactor.

2. PURPOSE

The purposes of this experiment are:

- Control rod calibration via stable period measurement:
  - Plot of the integral and differential control rod worths for different insertion levels of the CROCUS north control rod from period measurements.
  - A polynomial fit for reactivity vs. control rod position.
- Comparison of reactivity worths of the CROCUS north and south (reference) control rods.

3. SAFETY MEASURES

In order to work under the standard regulations for control of radiation exposure the safety measures and precautions during the experiment are:

- Personal dosimeter for each participant of the experiment (teachers, students and reactor operators) provided by the radiation safety group.
- Drinking and eating is not allowed in the control area.
- Do not move the control rods without authorization of the reactor operator.
- Start the data acquisition program at the same time as the control rod withdrawal.
- The initial transient region has to be assessed carefully and avoided for fitting.

4. INSTRUMENTS AND MATERIALS

This experiment measures the axial and radial flux distributions across the CROCUS reactor, therefore is done in the core of a nuclear reactor. It needs the following:

- The CROCUS reactor, critical at low power with partial insertion of the control rod to be calibrated
- Computerized system ("BABS") for the control rods movement
- DSA-1000 (multi-channel data acquisition system)
- PC and MATLAB based routines; available in the control room

Operational settings:

- Fission Chambers No. 1 & 2, DSA-1000 data acquisition systems from CANBERRA used in MCS mode and computers for recording the flux as a function of time.
- In the DSA-1000, the "Gamma Acquisition Analysis" (GENIE-2000) software is used. Basically, the following has to be done:
  - Start the GENIE-2000 program and then, launch the needed configuration: Open-source → Select DET#01 → count vs. time window appears
  - Open in MCA tab → Adjust → MCS

  There, the "dwell time" can be adjusted. This corresponds to the time interval per channel for data acquisition. There are 8192 channels in the DSA-1000. The total counting time has to be set such that this is sufficient to record, in an adequate manner, the increase of power consecutive to the withdrawal of the control rod.

5. EXPERIMENTAL PROCEDURES

- Starting with a critical reactor at low power (operator).
- Insert the control rod to the desired position, with the help of the reactor operator. The second control rod will be adjusted accordingly to have CROCUS critical. Ask authorisation of the reactor operator before any withdrawal of the control rod.
- Apply operational settings for the fission Chambers No. 1 & 2, DSA-1000 data acquisition systems from CANBERRA used in MCS mode and computers for recording the flux as a function of time.
- In the DSA-1000, the "Gamma Acquisition Analysis" (GENIE-2000) software is used. Basically, the following has to be done:
  - Start the GENIE-2000 program and then, launch the needed configuration: Open-source → Select DET#01 → count vs. time window appears
  - Open in MCA tab → Adjust → MCS

There, the “dwell time” can be adjusted. This corresponds to the time interval per channel for data acquisition. There are 8192 channels in the DSA-1000. The total counting time has to be set such that this is sufficient to record, in an adequate manner, the increase of power consecutive to the withdrawal of the control rod.

- Make sure the acquisition system is ready with a dwell time chosen for recording the power increase in an appropriate manner. (An estimate of the expected reactor period can be made on the basis of Table 4 and Fig. 5).

- Acquire the fission chamber counts rates per dwell-time channel for a sufficient period of time (usually over 2 decades of change in power, typically in the power range 0.1W to 20W).

- At the end of the power excursion, the operator will insert the control rods in order to lower the power and to prepare for the next measurement. Stop the acquisition system and save the measurement in the *.TKA format (ASCII). Keep a record of the control rod positions and the dwell time.

- Perform the data analysis with the MATLAB based executable or your own program using the provided kinetics parameters in Table 5.

- Repeat (3-5 times, depending of the time available) this procedure for another position of insertion of the control rod. Do not take several measurements for an insertion level higher than 500 mm (long reactor period), due to the time constraint.

6. MAIN PARAMETERS MEASURED

In order to obtain the integral and differential control rod worths for different levels of insertion of the calibrated control rod from period measurements, it is necessary to collect the following data:

- The fission chamber responses for different levels of insertion of the control rod.

- Mark the control rod position and dwell time used for each measurement.

7. TYPICAL REAL DATA COLLECTED

Examples of the typical real data collected:

The recorded dwell-times for each measurement step of the experiment are summarized in Table 1:

Table 1 Dwell times of the measured steps

Height of the control rod SOUTH in the reactor core [mm]	Dwell time [ms]
350	400
450	100
550	40
650	40
750	40
850	40
950	20

Fig. 4 shows a typical measured data in GENIE 2000 software with a dwell time of 2 s for all seven measured heights of the control rod in the reactor core as indicated in Table 1. The order of the measured steps was as follow: 450 mm, 550 mm, 650 mm, 750 mm, 850 mm, 950 mm and 350 mm.

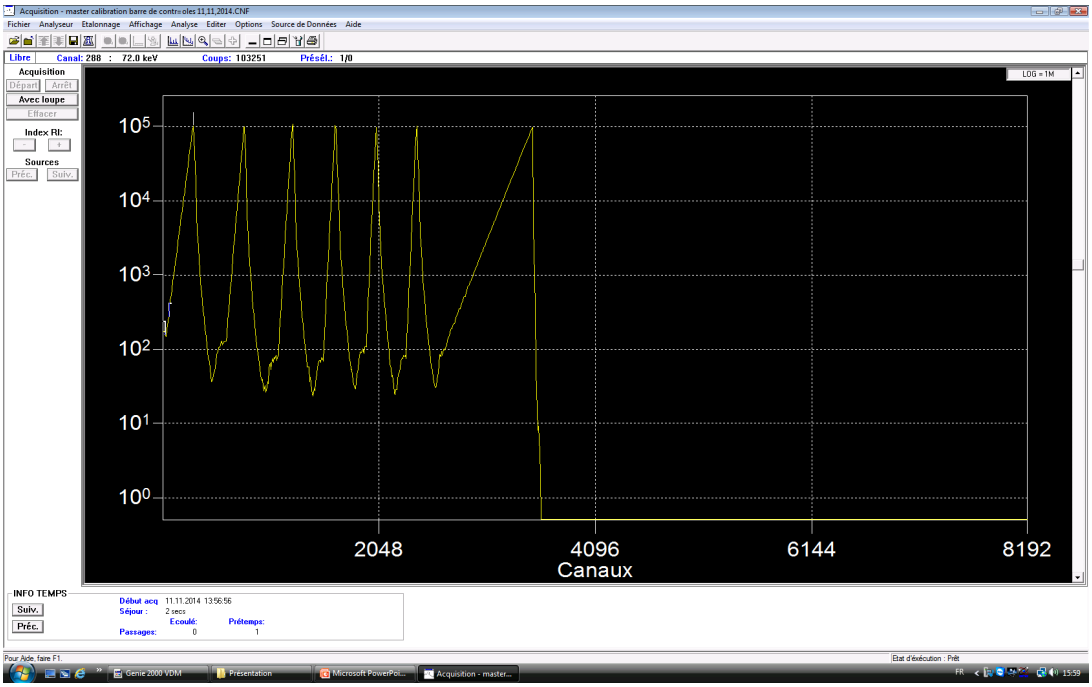

Fig. 4: Data acquisition of all seven measuring steps in GENIE 2000.

The *.TKA format (ASCII) output files from the acquisition system (GENIE 2000) with the fission chamber responses for different levels of insertion of the control rod are collected.

8. DATA ANALYSIS, ASSUMPTIONS AND EQUATIONS

Data Analysis:

- Run the MATLAB function, for instance "data.control.rod.exe" in the same directory as the data are being saved.
- Provide the necessary values in the dialog box, especially the file name, the dwell time used for the measurement and the desired output file.
- The output provides, among other things, the reactor period. Calculate the control rod worth from Equation (10) and the data provided in Table 5, see Section 8.
- Make a polynomial fit to the measured values of reactivity vs. rod position and compare the results with the data provided for the reference (calibrated) control rod.

Assumptions:

- The power level range for measurements is in the range of 100 mW to about 20 W.
- The reactivity worth of 40 mm of water (beyond critical water level) is equal to +200 pcm, the maximal allowed and possible positive reactivity in CROCUS.
- The total reactivity worth of a control rod is ~160 pcm.
- Specifications for the B_4C pellets and other details of the control rods are presented in Tables 2 & 3, respectively.

Table 2 Geometry and material characteristics of the B_4C pellets.

Description	B_4C pellet	σ_t at 0.025eV
Pellet diameter [mm]	8.5	-
B^{10} [%, barn-JEF-2.2]	19.9	3842.1
B^{11} [%,barn- JEF-2.2]	80.1	4.85
C^{12} [%, barn-JENDL-3.2]	98.9	4.8
C^{13} [%]	1.1	-

Table 3 Geometry of the control rods and guide tubes.

Description	Guide tube	Inner tube for holding pellets	Outer tube of the control rod
Material	Al 99.5	stainless steel	stainless steel
External ∅ [mm]	19.3	16.0	9.6
Internal ∅ [mm]	17.4	12.0	8.7

- The CROCUS control rods are referred to as NORTH and SOUTH control rods. The reactivity-worth curve (or "S-curve") of the south control rod has been determined

accurately and may be used as a reference for comparing the results obtained for the rod to be calibrated (NORTH). A polynomial fit to the measured reactivity worth of the south control rod is given by [3]:

$$\rho(x) = -192.39x^6 + 1690.9x^5 - 3473.6x^4 + 2363.3x^3 - 260.91x^2 + 37.974x - 0.001$$

where the reactivity worth $\rho(x)$ is in pcm (10^{-5}) and x is expressed in meters. Reactivity values
calculated from the fit are given in the Table 4.

Table 4 Reactivity worth of the 'SOUTH' control rod of the CROCUS reactor for different insertions (obtained from the polynomial fit to measured values).

Insertion length [m]	**Reactivity worth [pcm]**
0.2	11
0.4	52
0.6	112
0.8	154
1.0	165

- The kinetics parameters for the CROCUS reactor, required for the control rod calibration, are summarised in Table 5. These values correspond to mean values reported in the course of a numerical benchmark exercise for kinetics parameter calculations [4].

Table 5 Kinetics parameters for the CROCUS reactor. The table lists the mean values of the different calculated results reported in [4].

Λ = 5.93E-05 s		
Delayed neutron group	β_i **[-]**	λ_i **[s^{-1}]**
1	2.426E-04	1.291E-02
2	1.452E-03	3.138E-02
3	1.353E-03	1.187E-01
4	2.963E-03	3.163E-01
5	1.103E-03	1.197
6	3.468E-04	3.495
Total	7.460E-03	-

- It is seen, from Table 5, that the total delayed neutron fraction (β) for CROCUS is about 0.75%, i.e. considerably higher than 0.65%, the value for a purely ^{235}U-fuelled system. This is largely due to the fact that there is a significant contribution of fast fissions in ^{238}U, for which the delayed neutron fraction is as high as about 2%. The other contributing factor to the relatively large β-value of CROCUS is that delayed neutrons have a significantly lower average energy (~ 0.4 MeV) than prompt neutrons (~2 MeV). In a high-leakage core, such as CROCUS, there is consequently a preferentially higher leakage of prompt neutrons.

- The Reactivity Equation, Equation (10), can be used for calculating the stable reactor period ($T=1/\omega_1$) for any reactivity ρ introduced into a given reactor, on the basis of its kinetics parameters (Λ, β_i, λ_i).

- Fig. 5 provides, in graphical form, calculated results for the reactor period corresponding to a wide range of positive reactivity values (ρ) introduced into CROCUS. It is clear to see that the period becomes dangerously short as ρ approaches the delayed neutron fraction (β) of 0.75%, i.e. as ρ approaches the value of 1 dollar (the unit for reactivity, relative to the delayed neutron fraction). Prompt criticality ($\rho \geq \beta$) is a "forbidden" state for a reactor. As mentioned earlier, and as indicated in Fig. 5., the maximum permitted positive reactivity for CROCUS is 200pcm = 2.10^{-3} = (0.002/0.0075)$ = 27cents.

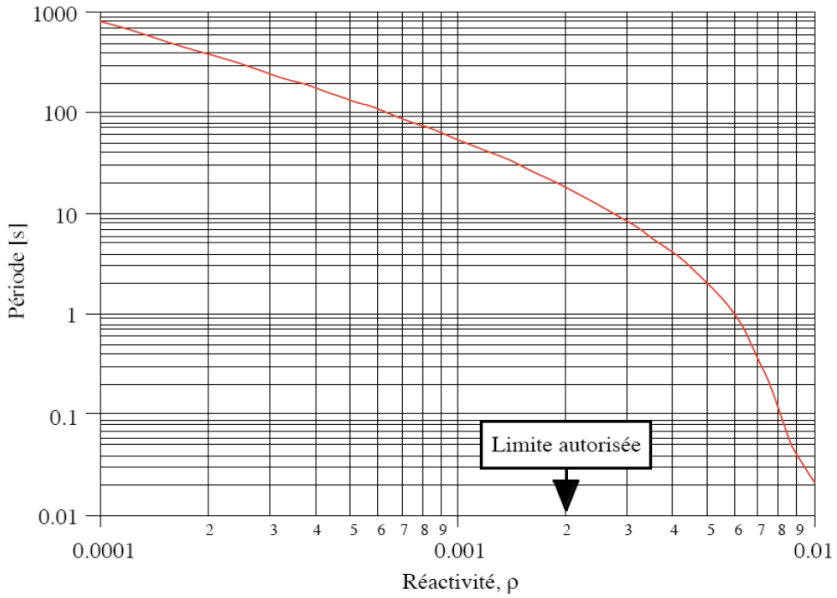

Fig. 5: Reactor period ($1/\omega_1$) vs. positive reactivity for the CROCUS reactor.

Sources of uncertainty:

- The uncertainty on control rod reactivity worth measured by asymptotic period, results from the combination of uncertainties on reactor period T and the kinetic parameters Λ, β_i, and λ_i (see Table 5). The first approach to the uncertainty analysis is based on the conventional uncertainty estimation, which approximates the function by a first-order Taylor series [5]. Both linearity and 'small' uncertainty are prerequisites of the conventional method of uncertainty estimation.

- Assuming no correlation between input parameters, the covariance terms are zero and the standard uncertainty in the reactivity can be estimated from the following expression:

$$\sigma_\rho = \sqrt{\left(\frac{\partial \rho}{\partial T}\right)^2 \sigma_T^2 + \left(\frac{\partial \rho}{\partial \Lambda}\right)^2 \sigma_\Lambda^2 + \sum_{i=1}^{n} \left(\frac{\partial \rho}{\partial \beta_i}\right)^2 \sigma_{\beta_i}^2 + \sum_{i=1}^{n} \left(\frac{\partial \rho}{\partial \lambda_i}\right)^2 \sigma_{\lambda_i}^2}$$

where σ_x represents the standard uncertainties associated with each input estimates x and the partial derivatives are called sensitivity coefficients. The evaluation of these sensitivity coefficients can be cumbersome for complex functions. For the Inhour equation $\varrho = f(T, \Lambda, \beta_i, \lambda_i)$ the standard uncertainty in reactivity with uncorrelated input parameters becomes:

$$\sigma_\rho = \sqrt{\left(\left(\sum_{i=1}^{n}\frac{\beta_i}{T^3\left(\lambda_i+\frac{1}{T}\right)^2}-\sum_{i=1}^{n}\frac{\beta_i}{T^2\left(\lambda_i+\frac{1}{T}\right)}-\frac{\Lambda}{T^2}\right).\sigma_T\right)^2+\left(\frac{1}{T}.\sigma_T\right)^2+\left(\sum_{i=1}^{n}\frac{1}{T\left(\lambda_i+\frac{1}{T}\right)}.\sigma_{\beta_i}\right)^2+\left(\sum_{i=1}^{n}-\frac{\beta_i}{T\left(\lambda_i+\frac{1}{T}\right)^2}.\sigma_{\lambda_i}\right)^2}$$

- When multiple measured input variables in a complex measurement system are correlated, uncertainty analysis becomes extremely difficult and sometimes even unreliable. The statistical sampling method is a practical alternative to the conventional method, and it is based on the propagation of probability distributions through a mathematical model for the evaluation of uncertainty. This applies to a model having any number of input quantities, and a single output quantity. In this alternative method, random numbers are used to randomly sample parameters uncertainty instead of point calculation carried out by conventional methods. Complex partial differentiations to determine the sensitivity coefficients are not necessary. It also takes care of input covariances or dependencies automatically [6].

9. PRE-KNOWLEDGE REQUIRED FROM STUDENTS

The students should be familiar with following contents:

- nuclear measurements: neutron detectors, basic experimental set up.
- reactor physics: neutron flux in a reactor, reactor kinetics, reactivity, stable period, control rod perturbations.
- radiation protection: dose rates, limits and all aspects regarding radiological protection, necessary to perform the experience under high security standards.

10.RESULTS

The measured data and corresponding fitting curves are displayed in the Fig. 6.

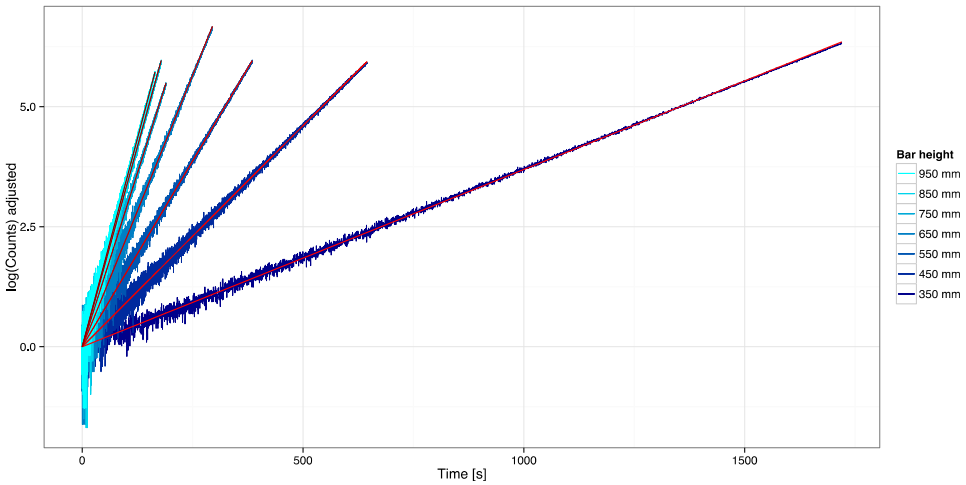

Fig.6: The measured data and corresponding fitting curves.

Table 6 shows determined values of ω as a function of the control rod's height.

Table 6 Approximated values of ω as a function of the control rod's height.

Height [mm]	350	450	550	650	750	850	950
ω	3.681E-03	9.203E-03	1.547E-02	2.261E-02	2.892E-02	3.331E-02	3.467E-02
σ_ω	0.002E-03	0.008E-03	0.002E-02	0.004E-02	0.004E-02	0.005E-02	0.005E-02

The reactivity of each measured step can be calculated based on ω - values from Table 6 using the 'Inhour Equation' (10). The calculated reactivity is shown in Fig. 7. The data are fitted with a sixth order polynomial

$$model(x)=ax^6+bx^5+cx^4+dx^3+ex^2+fx+g$$

with the following coefficients summarized in Table 7:

Table 7 Approximated values of the fitting parameters of the "S-curve".

Coeff.	a	b	c	d	e	f	g
Value	$-2.077.10^{-19}$	$8.328.10^{-16}$	$-1.363.10^{-12}$	$1.159.10^{-6}$	$-5.412.10^{-7}$	$1.347.10^{-4}$	$-1.382.10^{-2}$

The fitting has no uncertainty on the coefficients because linear algebra proves the existence, accuracy and uniqueness of a sixth order polynomial to fit 7 roots.

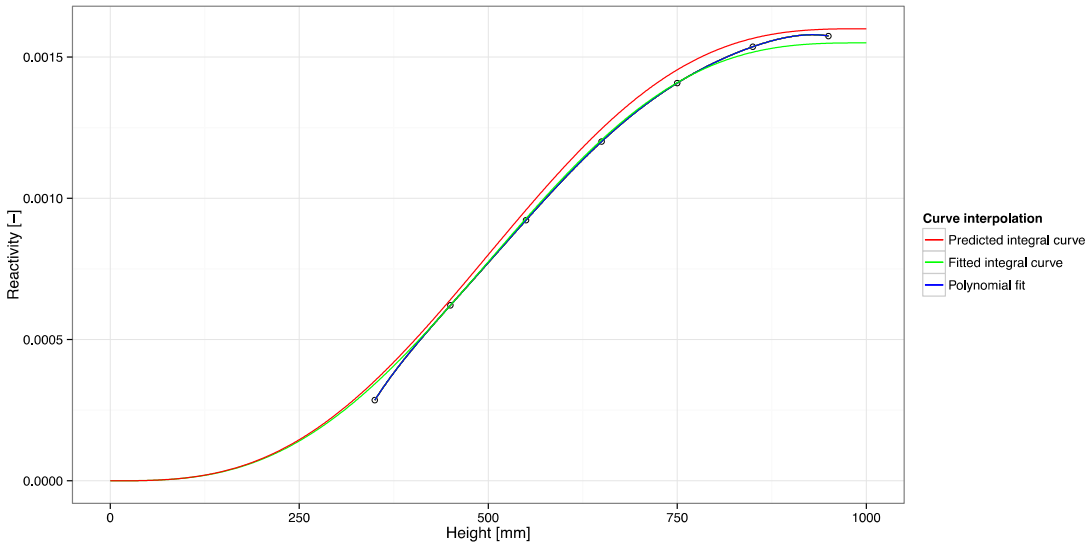

Fig. 7: Reactivity worth as a function of the SOUTH control rod's height.

Another interpolation is possible for the reactivity curve which fits also perfectly the experimental points and which is a better approximation of the physical reality for low values of the position. The differential reactivity, obtained by differentiating the integral fitting is shown in Fig. 8.

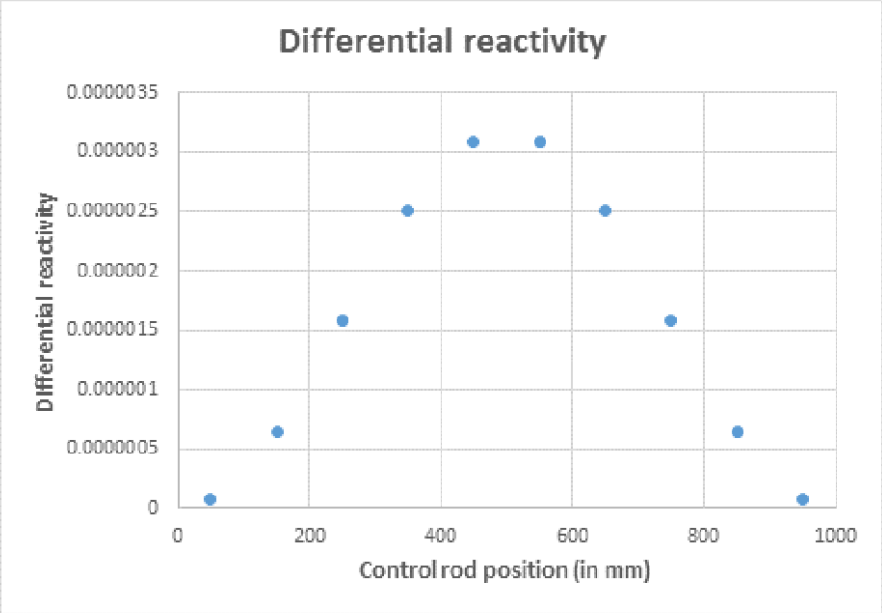

Fig. 8: Differential reactivity of the control rod in function of the its height.

A curve $\rho = f(z)$, one can compare and extrapolate as a *S*-shape curve, was determined in this experiment. Two parts can be underlined:

• The central "linear" part with an important slope: it means that in this region, with a small change of height, the reactivity can be quickly increased.

• The "flat" part close to a complete withdrawal: on a contrary, here, one needs to move a lot the control rod to increase the reactivity. From the integral curve, one can notice that the behaviour for low values of the position is similar.

The behaviour of the *S*-curve is directly linked to the differential reactivity shape.

11.CONCLUSIONS

The asymptotic period method was employed to measure the reactivity inserted by a fast step-like control rod withdrawal. Neutron population temporal evolution was measured using two ^{235}U fission chambers. For the given reactivity insertion, the neutron population asymptotically approached exponential growth at a rate given by the stable reactor period. Exponential fitting of the 'count rate vs. time' curves were used to extract the ω-values from the experimental data. The reactivity of each measured step was calculated based on those values by using the 'Inhour Equation'. The data were fitted with a sixth order polynomial and a typical S-curve for the CROCUS control rod (SOUTH) was obtained.

12.REFERENCES

[1] Lamarsh, J. R., “Introduction to Nuclear Reactor Theory”, Addison-Wesley, Reading Massachusetts, U.S.A, November 1972
[2] Keepin, R., ”Physics of Nuclear Kinetics”, Addison-Wesley Publishing company, Inc. Reading, Massachusettes, USA, 1965
[3] Girardin, G., ”Caractérisation d’une nouvelle paire de barres de contrôle pour le réacteur CROCUS de l’EPFL”, Travail de diplôme, EPFL, Février, 2004.
[4] Paratte, J.M., et al., ”A benchmark on the calculation of kinetic parameters based on reactivity effect experiments in the CROCUS reactor”, Annals of Nuclear Energy 33 (2006) 739-748
[5] Bureau International des Poids et Mesures, Commission électrotechnique internationale, and Organisation internationale de normalisation, “Guide to the Expression of Uncertainty in Measurement. International Organization for Standardization”, 1995.
[6] Bureau International des Poids et Mesures, Commission électrotechnique internationale, and Organisation internationale de normalisation, “Guide to the Expression of Uncertainty in Measurement Propagation of distributions using a Monte Carlo method”, International Organization for Standardization, 1995.
[7] Joneja, O., Girardin, G., Frajtag, P., Perret, G., Hursin, M., and Chawla, R., “Reactor experiments course - theory and measurements”, 2014

NEUTRON NOISE MEASUREMENT

1. INTRODUCTION

1.1 Theoretical background

1.1.1 Reactivity and reactor kinetics

Safety and good operation of a reactor requires knowing and controlling the average time behavior of the neutron population. The neutrons time behavior is predicted using reactor kinetic equations. These equations express the neutron population as a function of neutronic and thermal-hydraulic parameters characteristic of the reactor. Among these parameters the reactivity ρ, which is the ratio of average neutron production to neutron absorption plus leakage, plays a key role.

In a zero-power reactor the thermal hydraulic feedbacks are negligible because of the low power. The time dependence of the neutron population is shown to be a sum of exponential terms $N(t) = \sum_j A_j \, e^{\omega_j t}$ whose ω_j are solutions of the in-hour equation (1):

$$\rho = \Lambda\omega + \sum_i \frac{\beta_i \, \omega}{\omega + \lambda_i} \qquad (1)$$

The time behavior of the reactor readily depends on:

- the reactivity ρ,
- the generation time Λ, which is the average time between the birth of a neutron and a fission event it may cause,
- and the delayed neutrons which are usually gathered in 6 groups "i" and characterized by their delayed neutron fractions β_i and decay constants λ_i.

As an example, the reactivity is plotted in Fig. 1 as a function of the inverse period ω using delayed neutron data and a generation time typical for the CROCUS reactor. The curve exhibits 6 singularities corresponding to the values $-\lambda_i$ and there is 7 inverse periods ω_j solutions of a reactor having a given reactivity ρ/β, one associated with the prompt neutrons and six associated with the six delayed neutron groups. For a sub-critical reactor all seven values ω_j are negative. The smaller inverse period (on the left) is the one associated with the prompt neutrons. The term due to the prompt neutrons decay rapidly in a sub-critical reactor and the rate of decay depends of the reactivity. The larger inverse period (on the right) is still negative, reach zero for a critical reactor and becomes positive if the reactor is super-critical. This value is associated with the inverse asymptotic period of the reactor and governs the trend in the neutron population in the longer run.

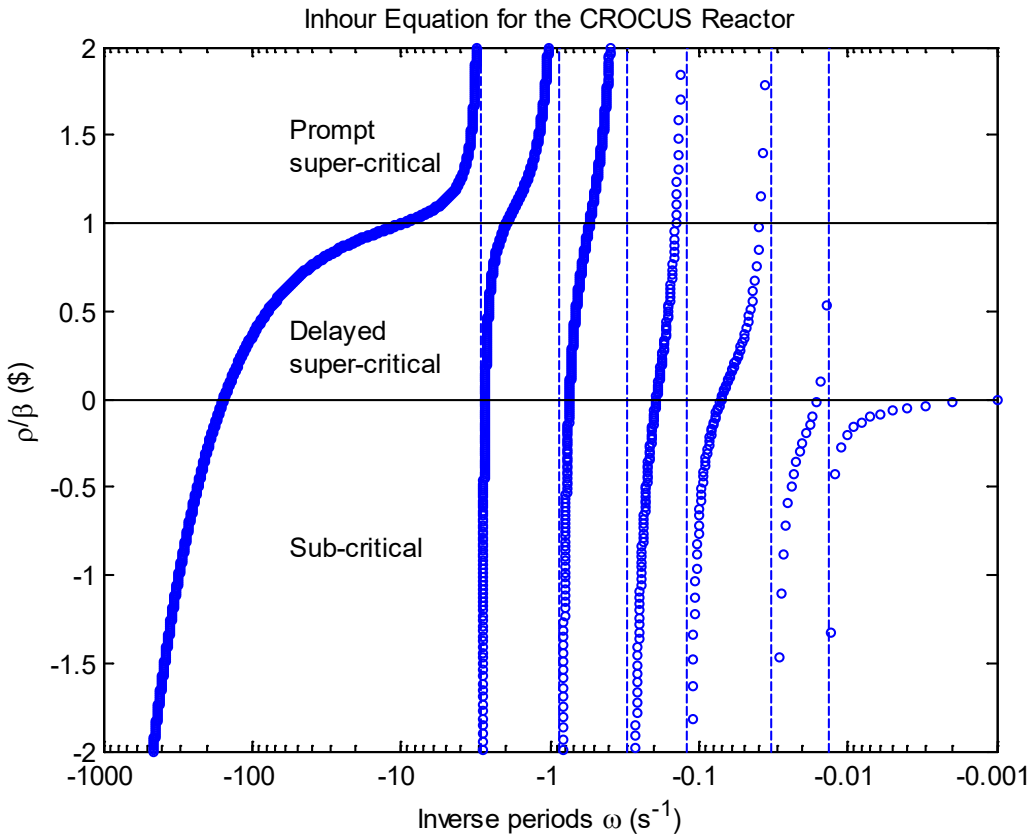

Fig. 1: Plot of the In-hour equation to quantify the decay constants of the neutron population following the insertion of a reactivity ρ.

As illustrated above, the determination of ρ, $\beta = \sum \beta_i$ and Λ is of critical importance. The parameters can be inferred experimentally by inducing a transient in the reactor (e.g. moving an absorber rod) and recording the evolution of the neutron population. Another less intrusive method consists in measuring the microscopic fluctuations of the neutron population in a macroscopically stable reactor. This method is far less intrusive and is the subject of the experiment.

1.1.2 Probability distributions, variances of signals

Microscopic fluctuations of the neutron population can be measured by plotting a histogram of the detected neutron signal.

The histogram is typically obtained after discretization of the signal in a multi-channel scaler (MCS), i.e. after its subdivision in consecutive time channels of constant length T. Each channel has a value x and the histogram is the plot of the number of channels n having the same values x as a function of x (see Fig. 2). It is a measurement of the probability distribution of the signal or more exactly of its probability density function (pdf), [1].

In some neutron noise techniques we do not need to know the full probability density, but only its average and variance (e.g. Feynman method). These quantities can be determined from the discretized signal $X = \{x_1, x_2, \dots, x_N\}$ by $E(X) = \frac{1}{N} \sum_{i=1}^{N} x_i$ and $Var(X) = \frac{1}{N} \sum_{i=1}^{N} {x_i}^2 - \left(\frac{1}{N} \sum_{i=1}^{N} x_i\right)^2$.

1	5	12	1	3	7	2	10	6	3

6	3

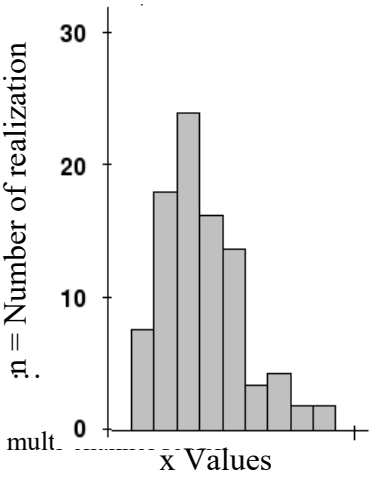

Fig. 2: Histogram plot of a time dependent signal discretized in a mult

Mathematically the relative likelihood of a continuous random variable X is given by its probability density function (pdf) $f_X(x)$. If the variable X can only take discrete values the relative likelihood is given by the probability mass function (pmf) $g_X(x)$. If the expression of the pdf/pmf is known, then the mean and variance can be obtained as:

$$E(X) = \int x\, f_X(x)\, dx \quad \text{and} \quad Var(X) = \int x^2\, f_X(x) dx - \left(\int x\, f_X(x)\, dx\right)^2$$

$$E(X) = \sum x\, g_X(x) \quad \text{and} \quad Var(X) = \sum x^2\, g_X(x) - \left(\sum x\, g_X(x)\right)^2$$

1.1.3 Characterisation of the count rate statistical distributions in a multiplying media such as CROCUS

In a multiplying media, such as a reactor, the probability distribution of the detected neutrons is more complex than in a non-multiplying media. In a reactor we have for example to account for fission events (generating 1 to 5 neutrons), capture events (eliminating one neutron) and the neutrons coming from a start-up or external source.

As an illustration Fig. 3 shows a neutron chain in blue. The neutron chain has fission (f), captures (c) and detection (d) events. The exact detection time is shown on the uppermost time scale. Using these time the histogram of time differences between the detections can be plotted. For example, with the neutron chain of Fig. 3, the channel T_b-T_a, T_c-T_a and T_c-T_b of the histogram would be incremented. It can be intuitively understand than the probability to detect two neutrons from the same neutron chain will not remain constant with the time difference between the detection. And that the time behaviour of the histogram might be characteristics of the reactor, for example of the average time between fission events or between fission and capture in a neutron chain.

This method is the Rossi-α method and is actually used in practice. It has been showed that, indeed, the histogram of time difference is of the form $f(T) = Ae^{\alpha T} + B$ where $\alpha = (\rho-\beta)/\Lambda$ is the prompt decay constant and T is the time difference between two detections [2]. The term $Ae^{\alpha T}$ characterizes detections of two neutrons belonging to the same neutron chain (as in Fig. 3). It varies with T and is for example decaying in time in a subcritical reactor. The second term is constant and characterizes the detection of two neutrons belonging to two different neutron chains.

T_aT_b T_c

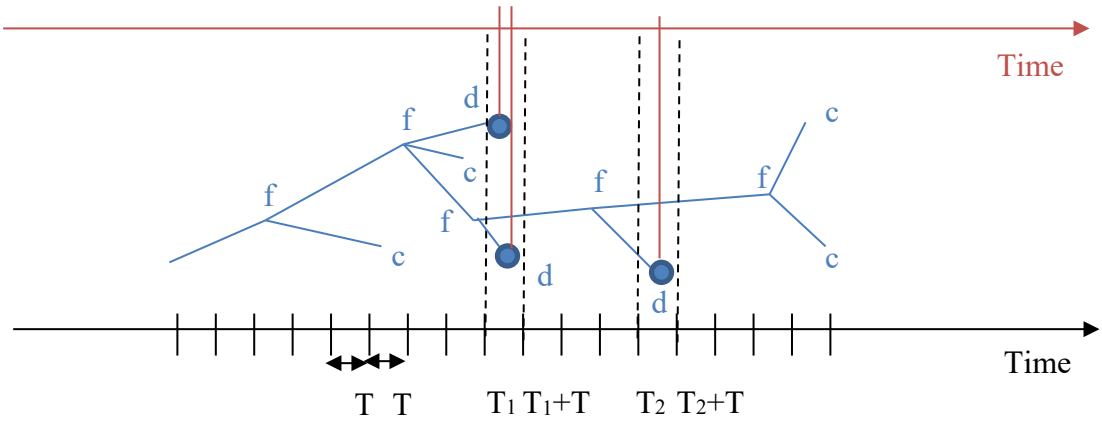

Fig. 3: Example of neutron chains with fission, capture and detection events.

Another way to characterize the probability distribution of the detected neutrons is to plot its variance-to-mean ratio (as for measurement 1). Using the lower time scale of Fig. 3, we can subdivide the time in equal chunks of length T, discretize the signal on it and compute the variance and mean. By repeating the same operation for different dwell time T we can obtain a curve Y(T).

Again from Fig. 3 one could expect that the variance and mean will vary with T and quantify the neutron chain properties in the reactor. This method is Feynman-α method and its theoretical expression for a single detector is [2]:

$$Y_{var}(T) = \frac{Var(T)}{mean(T)} - 1 = \frac{\epsilon\, D}{(\beta-\rho)^2}\left(1 + \frac{1-e^{\alpha T}}{\alpha T}\right) - 2Rd \qquad (2)$$

where T is the time length of the channel, ε is the detector efficiency i.e. the number of counts per fission in the core, $D = \langle \nu(\nu-1)\rangle / \langle \nu \rangle^2$ is the Diven factor, β is the delayed neutron fraction, ρ the reactivity, α = (ρ-β)/Λ the decay constant, d the detector dead-time and R the average detector count rate.

When two detectors are available, we can synchronize them and measure their covariance. This results in a formula featuring the two detector efficiencies ε_1 and ε_2 and the same reactor parameters [2]:

$$Y_{cov1,2}(T) = \frac{Cov1,2(T)}{\sqrt{mean_1(T)\, mean_2(T)}} = \frac{\sqrt{\epsilon_1 \epsilon_2}\, D}{(\beta-\rho)^2}\left(1 + \frac{1-e^{\alpha T}}{\alpha T}\right) \qquad (3)$$

Equations (2) and (3) are valid only if the time length T is small enough for the delayed neutrons to have a negligible influence because we are just characterizing the variance and covariance between prompt neutrons. As can be seen from Fig. 1, this requires the inverse period to be larger (in absolute value) to about 3 s^{-1}, i.e. a time constant T < 0.1s.

2. PURPOSE

The purposes of this experiment are:

- Characterization of the count rate statistical distributions in non-multiplying media:
  Characterize the statistical distribution of the gamma-ray emitted by a Co-60 source and detected by a sodium iodine detector facing the source.

- Characterization of the count rate statistical distributions in a multiplying media such as CROCUS:
  Characterize the statistical distribution of the neutrons in the reactor using its variance and its mean and infer parameters of the reactor such as the decay constant $\alpha = (\rho_{\$} + \beta)/\Lambda$.

3. SAFETY MEASURES

In order to work under the standard regulations for control of radiation exposure the safety measures during the experiment are:

- Personal dosimeter for each participant of the experiment (teachers, students and reactor operators) provided by the radiation safety group.
- Drinking and eating is not allowed in the control area.
- Use lab coat and gloves for the manipulation of the lead container with the Co-60 source in the CROCUS reactor hall.

4. INSTRUMENTS AND MATERIALS

Characterization of the count rate statistical distributions in non-multiplying media

- A sodium iodine (NaI) detector positioned in front of a ^{60}Co source.
- The detector is connected to an OSPREY combined pre-amplifier/amplifier unit which sends the signal via USB to the Multi-Channel Analysis (MCA) program GENIE2000 on the PC in the control room [3].
- The pre-amplifier and amplifier shape the detector signal such that the GENIE2000 can order and display the signal. It operates in two modes: Pulse Height Analysis (PHA) and Multi-Channel Scaler (MCS). The PHA mode is designed to record the number of gamma-rays as a function of their energy (summed during the whole measurement time), whereas the MCS mode records the number of gamma-rays in a given energy range as a function of time. In the MCS mode, the duration of each time channel is the same and is named the dwell time "dt". It can be adjusted from some micro seconds to some seconds, depending on the precision desired by the experimentalist. The total number of time channel available can also be adjusted from 128 to 65356 in order to have a recorded time sequence of the desired length.

Characterization of the count rate statistical distributions in multiplying media

- The CROCUS reactor at the critical state with a power of 50 mW.
- The instrumentation is similar to that of the measurement in non-multiplying media.
- Four neutron detectors (BF_3) inserted in the CROCUS core in the position shown in Fig. 4 - left (Periphery 1, 2 and CR1 and 2), connected to pre-amplifiers, amplifiers, discriminators (Fig. 4 – right), and fed to four multi-channel scaler (MCS) cards installed at the back of the acquisition PC.

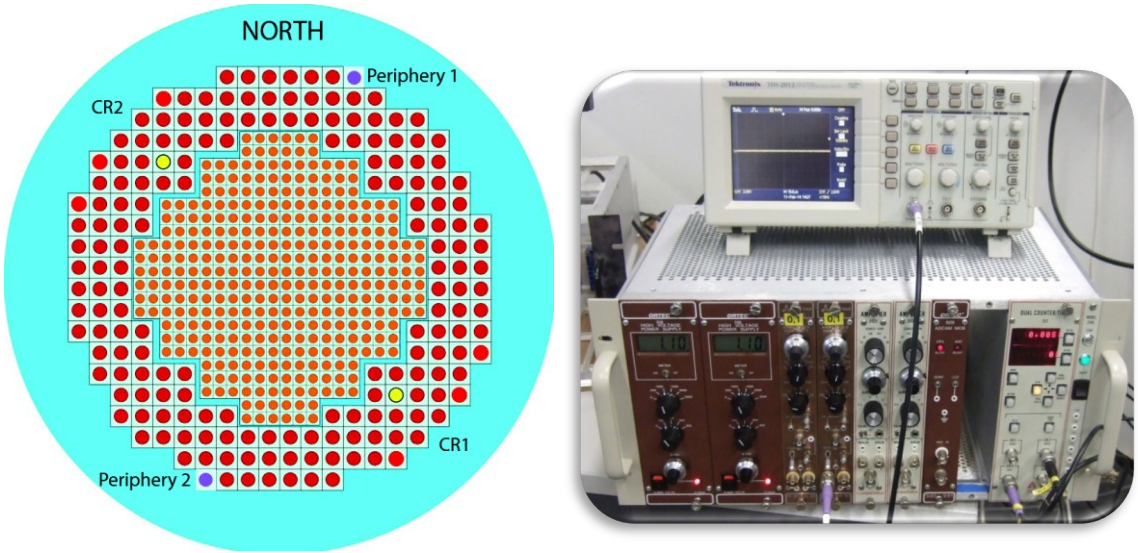

Fig. 4: Position of the detectors in CROCUS (left) and electronics used in the acquisition (right)

- The detectors identification numbers, their locations, the used cables, the amplifier model, the MCS-cards and the acquisition channels are summarized in Table 1.

Table 1 Set-up of the detectors and instrumentations

Detector	Core Position	Cables from Reactor (Channel #)	Amplifier	MCS Card
G45006	CR1	Blue (1)	ORTEC 572	MCB-121
G47349	Periphery 1	Black (2)	ORTEC 572	MCB-122
G45269	CR2	Yellow (3)	CANBERRA 2022	MCB-123
G45270	Periphery 2	Blue (4)	CANBERRA 2022	MCB-124

- The detector high voltage is provided by two ORTEC 556 units and is to be set to 1100 V. The ORTEC 572 and CANBERRA 2022 amplifier have a coarse gain of 10, a fine gain of 0.8 and a shaping time of 0.5 μs. The coarse gain potentiometer is set to 100 due to an internal gain multiplication factor of 0.1 in the ORTEC572 Amplifier.

5. EXPERIMENTAL PROCEDURES

Characterization of the count rate statistical distributions in non-multiplying media

1. Log as "Master Experiment" User (no password) on the Neutron Noise Measurement PC in the CROCUS reactor hall.
2. Launch the program GENIE2000 on the PC – the manual is available on the desktop for more information [3].
3. Open the local detector DET01.08 (File Menu/Open Datasource/Detector, see [3] p. 41).
4. Power the detector high voltage at 400V (MCA Menu/Adjust/HPVPS, see [3] p. 56) and verify that the control LED on the PMT is on.
5. Take the ^{60}Co source #57, which had an activity of 37 MBq on the 31.12.1968 and place it at 5-6 cm from the surface of the detector.
6. What is the current activity of the source?
7. Measure the dose rate of the source with an ADC-6 in contact of the source and behind the lead bricks. How does it compare with the annual dose rate limit of 1 mSv/year for person non-exposed to radiation during their work?
8. Selection of the 1.33 MeV gamma-rays:
   8.1. Launch the acquisition and stop it after a minute.
   8.2. Observe the acquired spectra (number of counts as a function of the energy/channel). Comment on the spectra features.
   8.3. Note the channel delimiting the highest energy peak of the spectra
   8.4. Open the local detector as in step #1 but chose MCS instead of DET01.08
   8.5. Go to MCA Menu/Adjust/MCS and select Disc. Mode to ROI and input the noted channel numbers for the start and end of the ROI (see [3] pp. 58-59). Confirm each time by pressing OK. We are selecting only the highest energy gamma-rays for the recorded signal.
9. Set the dwell-time of the measurement to 0.1 s and start the acquisition and stop it after 3-5 minutes.
10. What is the signal behaviour?
11. Plot the histogram of the signal and determine its average and its variance. For this you can use Excel and the video instruction [4], whose link is also on the PC's desktop.

12. What probability density function (pdf) can be observed?
13. What are the variance, the mean and their ratio?
14. Repeat the measurement with a dwell time of 0.01 and 0.001 seconds. How those dwell times change the probability distribution and the variance-to-mean ratio?

Characterization of the count rate statistical distributions in multiplying media

1. Make CROCUS critical with a power of 50 mW without the start-up neutron source (operator).
2. Power ups the instrumentation and set parameters according to the settings given in the previous section (BE CAREFUL never to turn the high voltage of the detector on before turning on the low voltage of the pre-amplifier).
3. Test the detectors by observing the signal after the pre-amplifier and the amplifier using an oscilloscope.
4. Acquisition dry-run
    a. On the acquisition PC6010 open the folder Exp09 and launch the acquisition program "Slow_Acquisition.vi" in the folder Algorithm (see Fig. 5)
    b. Fill out the "Card Settings" block with the card names and threshold values shown in Fig. 5. It is important to select the card MCB121 as the card #1 (i.e. the master card). Set the dwell-time to 500 μs, the pass length (number of channel in the card) to 60 000 channels and the total number of sweep to 5.
    c. Fill out the "TDMS file Settings" block with the directory and root filename for the output (see Fig. 5 for an example).
    d. Click the right arrow below the Edit menu to activate the vi and start the acquisition by pressing the START button.
    e. Adjust the number of sweeps (i.e. repetition of the measurement) to have a total acquisition time of 30 minutes.
    f. After the acquisition is finished (LED finished on) open the .tdms files created for each card using the excel importer with aright click.
5. Acquisition
    a. Repeat step 4 but increasing the number of sweeps to measure during 30 minutes
6. Preparation of fit routines
    a. During the measurement, prepare the routines to fit the Feynman-α expression of Eq. (2) and (3 as a function of T in order to derive the decay constant value α and its uncertainty.
    b. Input data is in the form of three columns of number (T, Y(T), sigma(T)).
    c. Available programs are Excel, Matlab and Mathematica. If you are not familiar with any of these programs we suggest you to use either the "cftool" toolkit from MATLAB, which has a user-friendly GUI interface or Excel Solver add-ins (see Appendix D, [5]).
7. Post-processing of the data
    a. When the acquisition is finished launch the program "Y_Postprocessing.vi" in the folder Algorithm (see Fig. 6).
    b. Fill out the "Input Data" block to process the four cards.
    c. Don't resize the TDMS file, selecting a sweep and channel offset of 0.
    d. Chose the maximum number of grouped channels (Dwell Time) such that $T < 0.05$s.
    e. Activate the vi with the white arrow (below the Edit menu).
    f. TDMS and ASCII files have been created for the variance and covariances.

8. Share the variance and covariance results $\{Yvar_i\}_{i=1:4}$ and $\{Ycov_{1,i}\}_{i=1:4}$ between the two groups and fit the results with your routines.
9. What are the decay constants and their uncertainties? Are the results consistent with one another? How do they compare with the code predictions given in Appendix F, [5] ?
10. Derive the decay constant for all detectors (1+2+3+4) taken together $Yvar_{tot}$. Does the result improve?
11. Bonus questions:
    a. How would the Feynman-α curves change if the reactivity was lower (i.e. in sub-critical states)?
    b. Could you extract more characteristics of the reactor from the Feynman-α curves than just α assuming that you know the fission rate in the reactor?

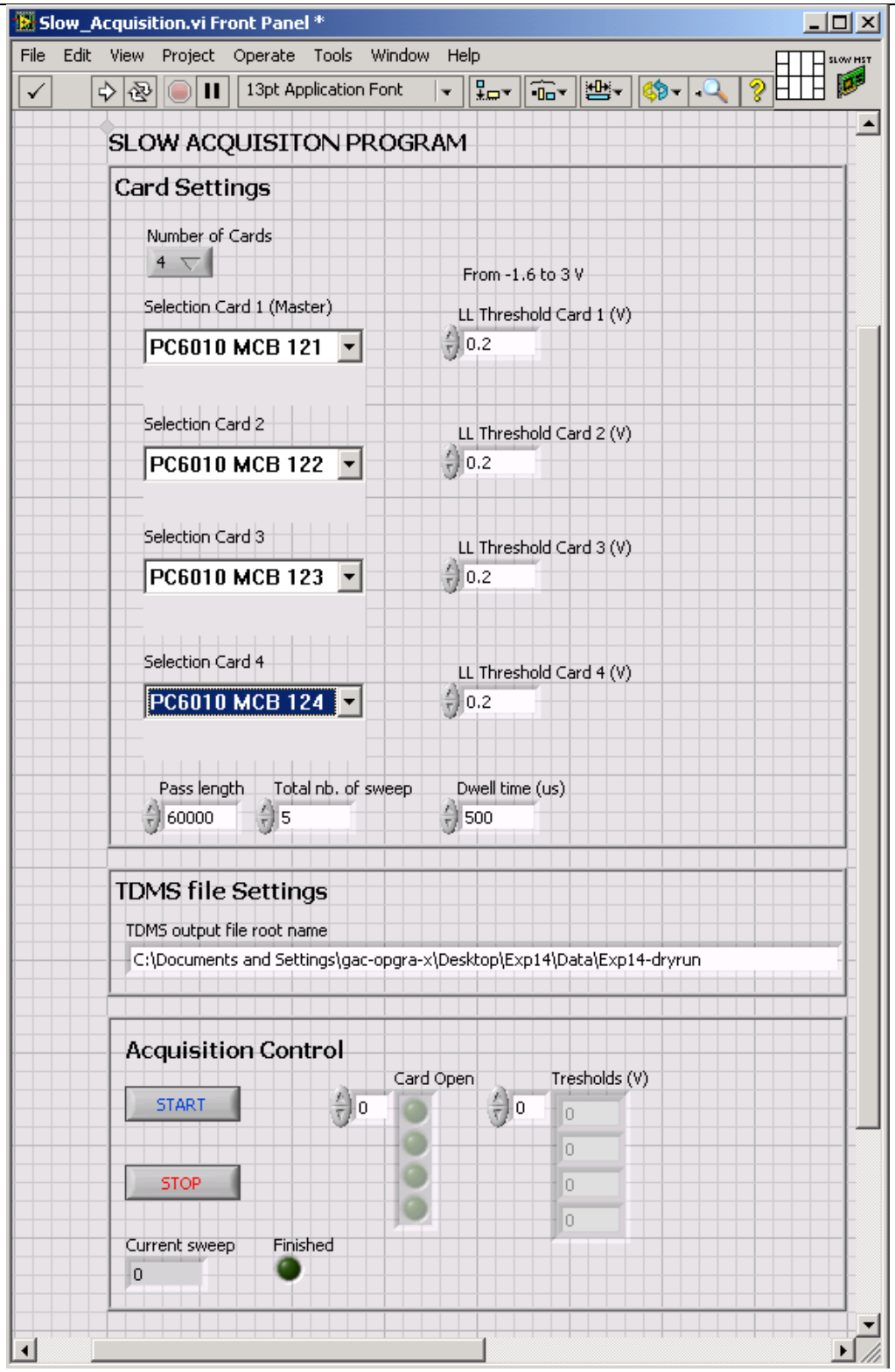

Fig. 5: Acquisition program front panel.

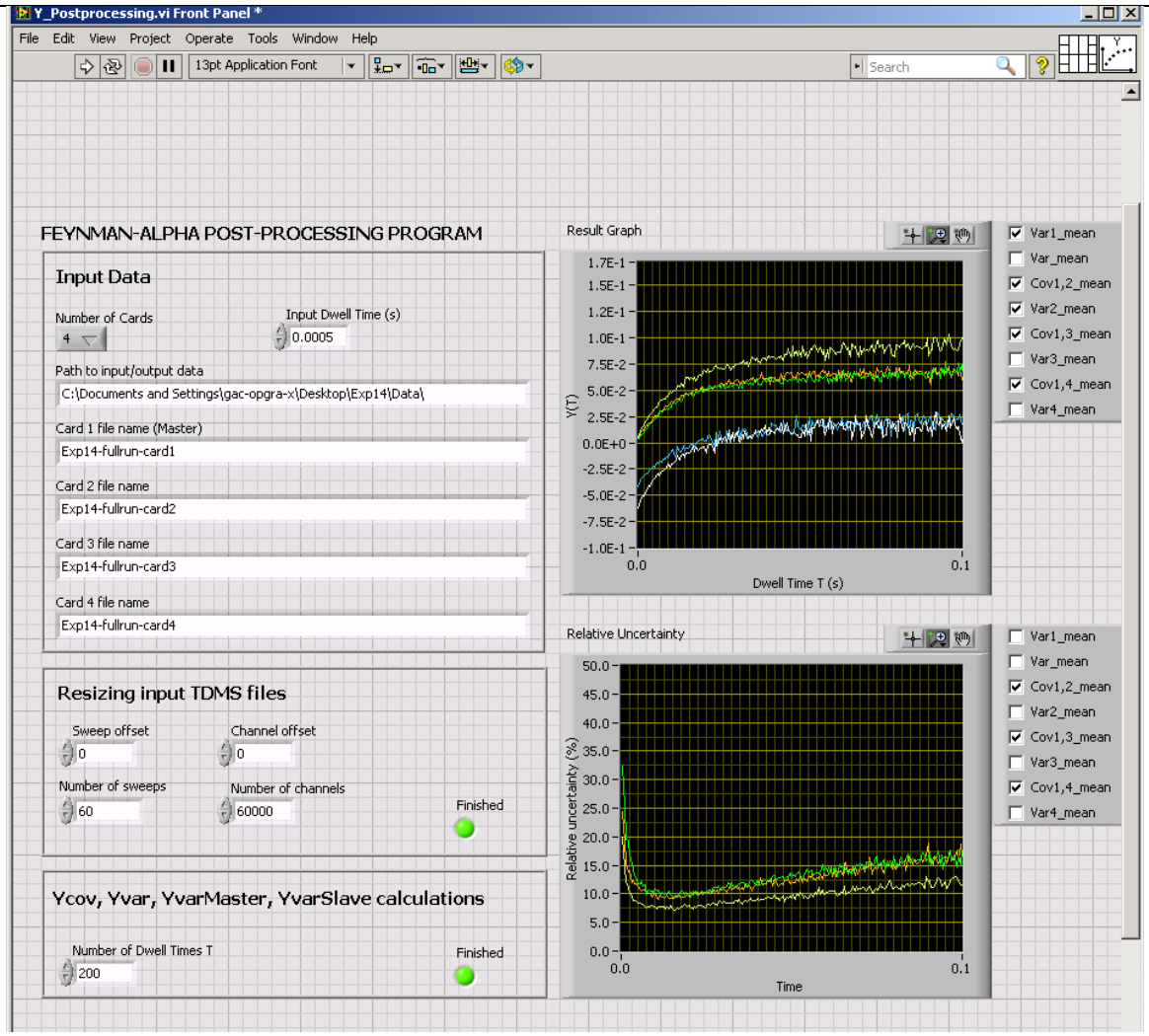

Fig. 9.6: Post-processing program front panel.

6. MAIN PARAMETERS MEASURED

Characterization of the count rate statistical distributions in non-multiplying media

- The PHA mode is used first to select the energy range of interest for the gamma-rays and then the MCS mode to record the time distribution of the gamma-ray signal. The probability distribution of the signal will be extracted from this time distribution.
-

Characterization of the count rate statistical distributions in multiplying media

- Theoretically, the measurements for different value of the channel width T is needed to be repeated. In practice, however, the measurement is done only once with a small value of T=dt (e.g. 500 μs). The adjacent channels of the MCS are then regrouped after the measurement to directly yield values for T=2dt, 3dt, 4dt, etc.

7. TYPICAL REAL DATA COLLECTED

Examples of the typical real data collected to obtain the count rate statistical distribution:

The count rate from an iodine crystal detector is measured, using different dwell times, i.e each channel of the analyser corresponds to a fixed period (=dwell time) and the graph displays the count rate (number of counts) for each channel.

The following Figs. 7 and 8 present the count rate histograms for different dwell times of 0.1 s, 0.01 s and 0.005 s. The x-axis corresponds to the different values of count rate during one period and the y-axis is the number of the realizations.

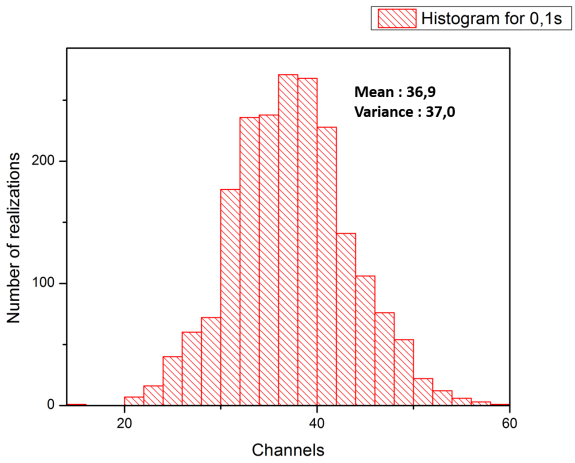

Fig. 7: Count rate histogram for a dwell time of 0.1s.

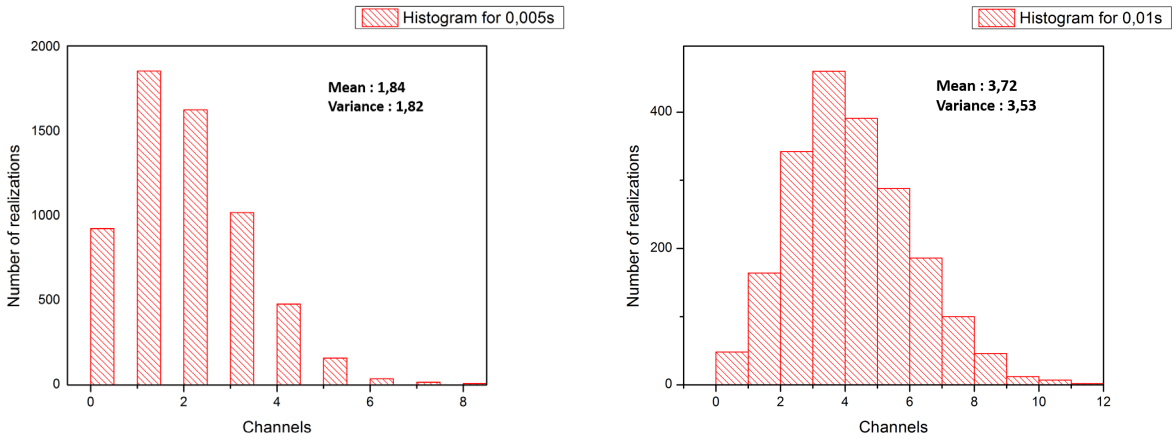

Fig. 8: (a) Count rate histogram for a dwell time of 0.01 s; (b) Count rate histogram for a dwell time of 0.005 s.

Examples of the statistical count rate distribution in CROCUS:

The following figures display Y_{var} (Fig. 9 and 10) and Y_{covar} (Fig. 11) versus time for the different detectors placed in the reactor core.

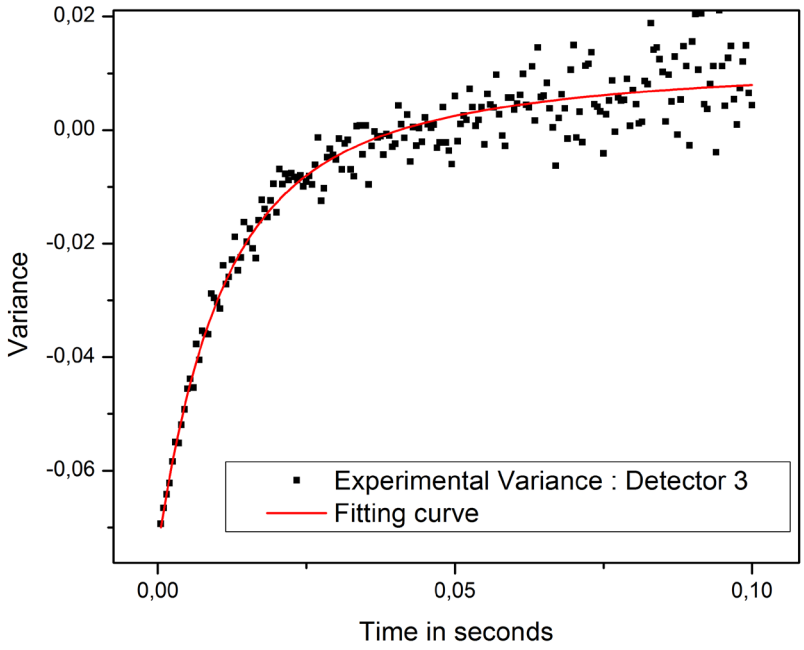

Fig. 9: Feynman-α method with the variance of the detector 3.

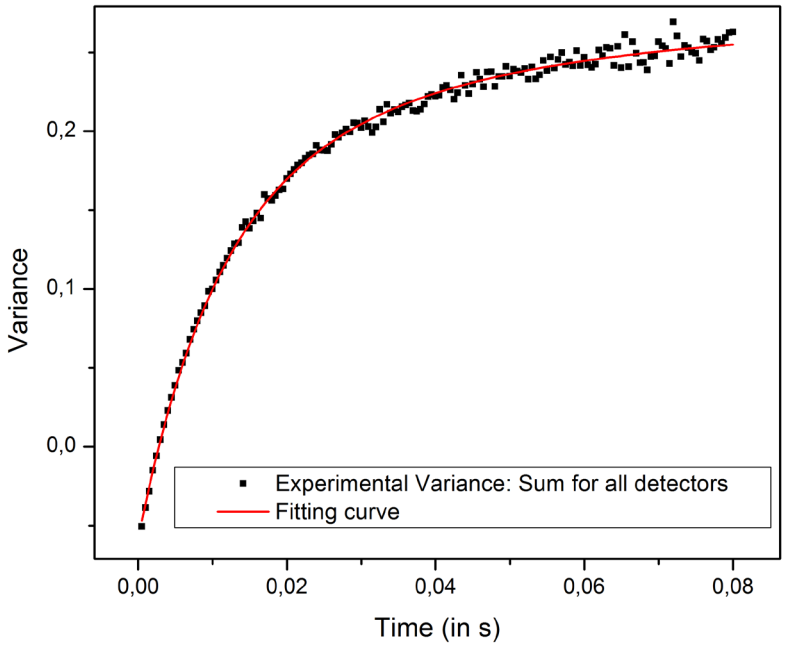

Fig. 10: Feynman-α method with the sum variance from all the detectors.

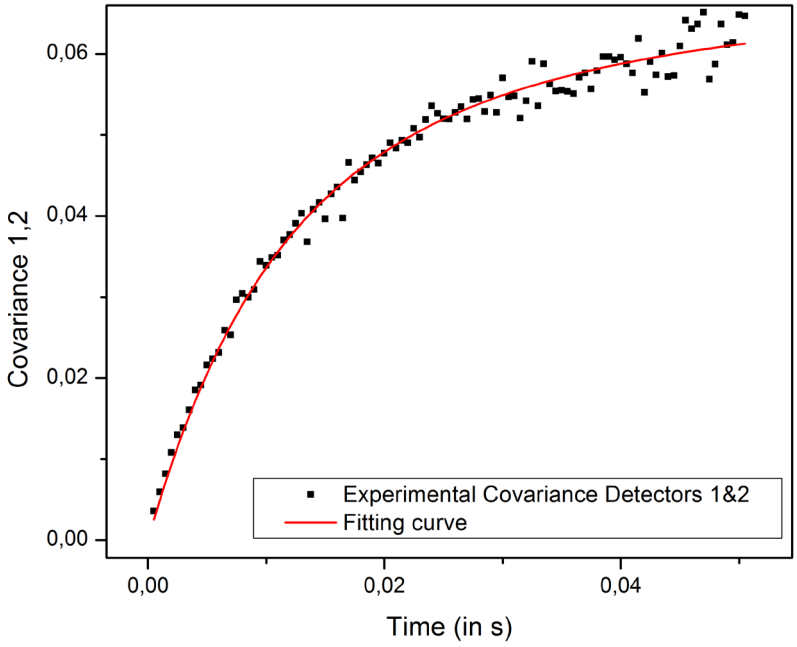

Fig. 11: Feynman-α method with the covariance between detectors 1 & 2.

8. DATA ANALYSIS, ASSUMPTIONS AND EQUATIONS

The first part of the experiment consists in demonstrating that the radioactive decay follows a Poisson distribution law:

$$P(N,t) = \frac{(\lambda t)^N}{N!} e^{-\lambda t}$$

The results demonstrate this assumption in a proper way. The histogram of the fluctuation for high dwell time doesn't show the Poisson characteristic of the emission, as the correlation between two successive events is lost. The Poisson distribution is revealed for dwell times, which are small enough compared to the count rate.

In a multiplying media, events can occur between the birth of a neutron and its detection, such as fission, capture or scattering. In order to determine the characteristic time of these events, the goal is to detect two events resulting from the same neutron chain. This can be performed by measuring the events recorded in given time steps. Intuitively, the probability to detect an event right after another event is detected should be higher, as the neutrons coming from the same chain reach the detector with a time lag related to their proximity in the chain (neutrons from the same disintegration may reach the detector with a very brief time lag). Apparently, for large time steps, this behaviour cannot be revealed, as the number of events detected is high due to the high uncorrelated events constant background. As the time step is reduced in order to get either zero or one event per step, then such a probability can be easily determined.

This is practically done using the Rossi-α or the Feynman-α methods, which model the described probability as a function of the time step. The latter is shown in the results section, as it is easily applied in practice: the variance of the signals mean is computed for different dwell time. This is performed for one single detector (Fig. 9) and all the four detectors (Fig. 10). Two observations can be made:

• The spreading of the points is less important for the two detectors, due to the larger amount of measurements reducing the uncertainty.

• The variance of the mean for both measurement is shifted to lower values by a constant parameter which is the expression of the dead time in the following equation:

$$\mathrm{Y}_{var}(\mathrm{T}) = \frac{Var(T)}{mean(T)} - 1 = \frac{\epsilon\, \mathrm{D}}{(\beta - \rho)^2}\left(1 + \frac{1 - \mathrm{e}^{\alpha \mathrm{T}}}{\alpha \mathrm{T}}\right) - 2Rd$$

For an extremely reactive detector without any dead time, the variance at an infinitesimal time step should be zero.

Another way to characterize the distribution is to synchronize the two detectors and measure their covariance on the mean for different time steps, as shown in Fig. 11. As it can be clearly seen on the graph, the constant term of the dead time does not contribute anymore, as the covariance is zero for an infinitesimal time step. The covariance has a constant asymptotic limit for large time step, which shows the constant non-correlated events background.

9. PRE-KNOWLEDGE REQUIRED FROM STUDENTS

The students should be familiar with following contents:

- nuclear measurements: instrumentation and data acquisition system (gamma and neutron detectors, basic experimental set up).
- reactor physics: neutron noise measurement theory, reactivity and reactor kinetics.
- probability distributions, variances of signals
- radiation protection: dose rates, limits and all aspects regarding radiological protection, necessary to perform the experience under high security standards.

10.RESULTS

The obtained distributions are fitted with the following expression:

$$Y_{var}(T) = \frac{Var(T)}{mean(T)} - 1 = A\left(1 + \frac{1 - e^{\alpha T}}{\alpha T}\right) - C$$

$$Y_{cov1,2}(T) = \frac{Cov1,2(T)}{\sqrt{mean_1(T)\, mean_2\,(T)}} = B\left(1 + \frac{1 - e^{\alpha T}}{\alpha T}\right)$$

The above two equations are valid only if the time length T is small enough to neglect the influence from delayed neutrons due to characterisation of the variance and covariance between prompt neutrons. Thus, all the fittings of measured data (Figs. 12-19) are exclusively applied to the time ranges of interest from 0.0005s to 0.05s, which give lower uncertainties. The following Table 2 lists all the derived values of the decay constant by fitting curves and their uncertainties obtained from the curve-fitting tool in MATLAB.

Table 2 Decay constant values and uncertainties

Detector:	**1**	**2**	**3**	**4**	**1,2**	**1,3**	**1,4**	**1,2,3,4**
α [s^{-1}]	-158	-142	-160	-126	-143	-150	-153	-130
σ_α [s^{-1}]	15	24	20	16	8	6	8	4

Decay constants derived from the fitting of measured data (Figs. 12-19) are consistent with each other. The results are within 1 or 2 standard deviations compared to the predicted value of (−154.4 ± 1.6) s^{-1} [6], which eliminate a significant systematic error of the method.

The position of the inserted detectors, detector 1 and detector 3 are almost placed symmetrically, which can account for the better consistency between detector 1 and detector 3, likewise to the detector 2 and detector 4. The decay constants derived from the covariance are more precise with lower uncertainties than using the variance for a single detector. However, the decay constant derived by taking all detectors together does not yield to a value with a better precision. Nevertheless, the uncertainty was lowered by this consideration.

Although, the predicted value of of $(-154.4 \pm 1.6)\ s^{-1}$ [6] is not within a few standard deviations of the obtained result, it can be assumed that this is due to the fact that results from single detectors were add up and treated effectively as one detector. Moreover, it is possible that the systematic error occurs in the simulation, as it can be seen that the symmetry between the detectors plays only a minor role and the noise measurements are indeed independent of symmetrical considerations.

In order to characterize the reactor with the decay constant and other parameters like A, B and C derived from the fitting equations, the reactor fission rate R has to be known. Then, the following relations can be used:

$$A = \frac{\epsilon D}{(\beta-\rho)^2};\ \ B = \frac{\sqrt{\epsilon_1 \epsilon_2} D}{(\beta-\rho)^2};\ \ \ C = 2Rd \longrightarrow\ (\beta-\varrho)^2 = \frac{\epsilon D}{A} = (\alpha\Lambda)^2,$$

where ε is the detector efficiency, the Diven factor D is known to be around 0.8 and d is the detector dead-time. Thus, we can easily determine the detector efficiency by the ratio of the measurement to the real neutron flux derived from the fission rate. Moreover, using the value of A and decay constant α, we can calculate the neutron generation time Λ. For a critical reactor the reactivity is zero, and then the delayed neutron fraction can also be calculated. Therefore, the reactor characteristics can be determined by measuring the neutron noise.

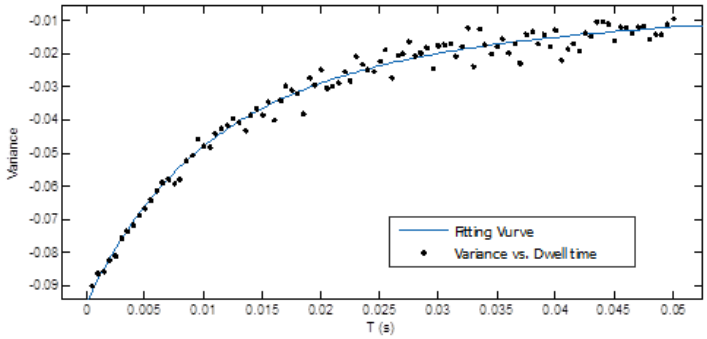

Fig. 12: Feynman-α method with the variance of the detector 1.

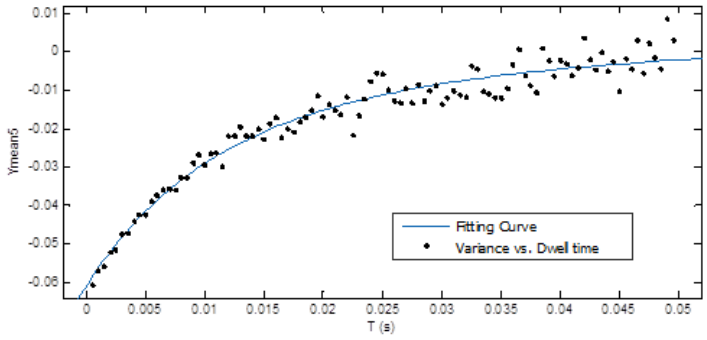

Fig. 13: Feynman-α method with the variance of the detector 2.

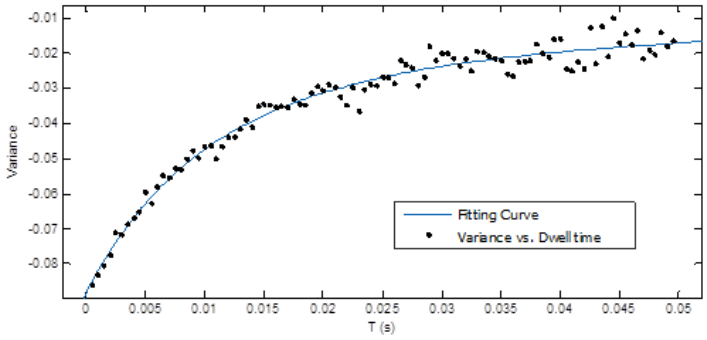

Fig. 14: Feynman-α method with the variance of the detector 3.

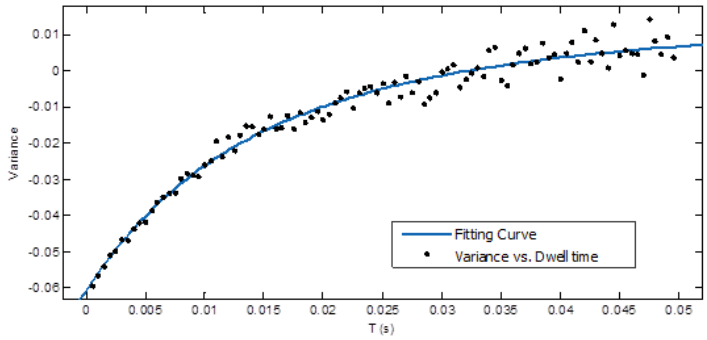

Fig. 15: Feynman-α method with the variance of the detector 4.

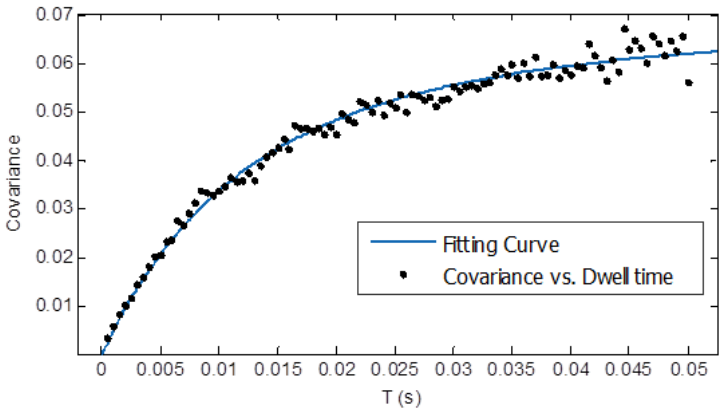

Fig. 16: Feynman-α method with the covariance between detectors 1 & 2.

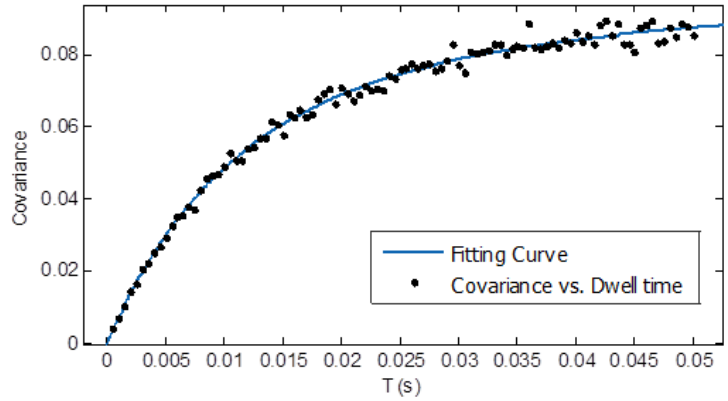

Fig. 17: Feynman-α method with the covariance between detectors 1 & 3.

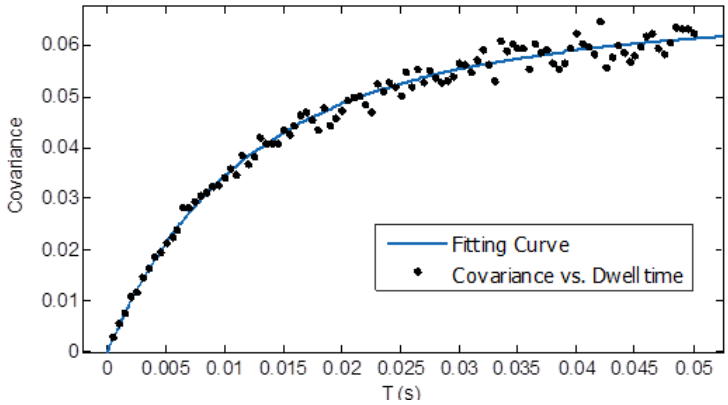

Fig. 18: Feynman-α method with the covariance between detectors 1 & 4.

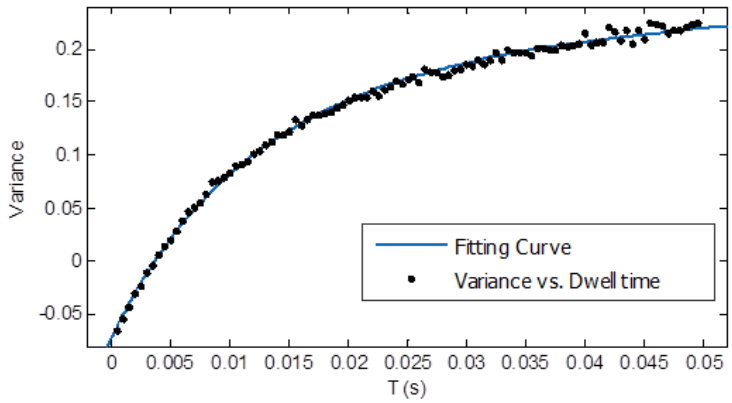

Fig. 19: Feynman-α method with the sum covariance from all the detectors.

11.CONCLUSIONS

The results obtained with the ^{60}Co source in a non-multiplying media are in accordance with the theory, as the emission distribution is found to follow a Poisson law. This result is analytically proven.

In a multiplying media, the total of eight sets of decay constants of the CROCUS reactor were derived. The decay constant value of (−153.0±8.0) s^{-1} was calculated from the covariance of the detector 1 and detector 4. This value is the closest to the predicted value of (-154.4±1.6) s^{-1}, [6]. The results obtained by summing up the measurements from all four BF_3 detectors - assuming that only one detector is present - were not in a better agreement with the simulated value. However, the uncertainty was lowered by this consideration.

This experiment proved that it is possible to characterize a reactor without any safety risks from intrusive means, i.e. moving control rods, but only by observing flux fluctuations and deriving their statistical properties. It is evident that the reactor tends to leave characteristic information about its properties in the neutron noise.

12.REFERENCES

[1] http://en.wikipedia.org/wiki/Probability_distribution
[2] Williams, M.M.R., Random Processes in Nuclear Reactors. Pergamon Press, Oxford, 1974
[3] http://www3.nd.edu/~wzech/Genie%202000%20Operations%20Manual.pdf
[4] https://www.youtube.com/watch?v=RyxPp22x9PU
[5] Joneja, O., Girardin, G., Frajtag, P., Perret, G., Hursin, M., and Chawla, R., "Reactor experiments course - theory and measurements", 2014
[6] Roland, V., Perret, G., Girardin, G., Frajtag, P., Pautz, A., "Neutron Noise Measurement in the CROCUS Reactor", Joint IGORR & IAEA Tech nical Meeting, Daejon, Korea, October 2013